Correlation effects, finite size, chemi-adsorption, and image charge effects in the macro-ion-electrolyte system: a field theoretic approach.

D. J. Lee*
Max-Planck Institut für Physik Komplexer Systeme, Nöthnizer Str.38, D-01187, Dresden, Germany

We consider a model of a macro-ion surrounded by small ions of an electrolyte solution. The finite size of ionic charge distributions of ions, chemi-adsorption and image charge effects are all considered. From such a model it is possible to construct a statistical field theory with a single fluctuating field and derive physical interpretations for both the mean field and two-point correlation function. For point like charges, without chemi-adsorption, at the level of a Gaussian (or saddle point) approximation, we recover the standard Poisson-Boltzmann equation. However, to include ionic correlation effects, as well as image charge effects of individual ions, we must go beyond this. From the field theory considered, it is possible to construct self-consistent approximations. We consider the simplest of these, namely the Hartree approximation. The Hartree equations take the form of two coupled equations. One is a modified Poisson-Boltzmann equation; the other describes both image charge effects on the individual ions, as well as correlations. Such equations are difficult to solve numerically, so we develop an (a WKB like) approximation for obtaining solutions. This, we apply to a uniformly charged rod in univalent electrolyte solution, for both extended spherically symmetric distributions of ionic charge on electrolyte ions, as well as for point like ions. The solutions show how finite size charge distributions of the ions reduce both the effects of correlations and image charge effects. We test the WKB approximation by calculating a leading order correction from the exact Hartree result, showing that the WKB like approximation works quite well in describing the full solution to the Hartree equations. From these solutions, we also calculate an effective charge compensation parameter in an analytical formula for the interaction of two charged cylinders.

1. Introduction

The mechanisms of interaction between cylindrical macro-ions in electrolyte solutions are still not fully understood [1]. The unmodified PB equation for a uniformly charged cylinder may be inadequate in describing the interaction for a variety of reasons. Correlation effects [1,2,3,4,5,6,7,8,9,10,11], image charge effects [1,5,8,10,12,13], solvent effects [12,14,15,16,17,18,19,20], and structure of charged groups at the macro-ion surface [1,12,20,21,22,23] may all play an important role. Though, the relative degree of each of these effects is likely to depend on the particular properties of the type macro-ion under consideration, most importantly its shape, charge density and surface charge distribution of fixed charged groups.

Correlation effects may lead to two predicted phenomena, that of charge inversion [1,7,24,25] and same charge attraction [1,3,5,7,9,11,26]. In charge inversion, the amount positive charge, due to counter-ions exceeds the surface charge density of the macro-ion effectively making it of opposite charge to its charged groups. Same charge attraction describes a situation in which two macro-ions of the same charge are able to attract each other through interactions with their counter-ions. Notably, both these phenomena have been predicted in the case of strong correlations between ions at the macro-ion surface

* Electronic mail: lee@mpipks-dresden.mpg.de or domolee@hotmail.com.

[7,6,26], where it supposed that a Wigner crystal forms on the surface of each macro-ion. Here, the mechanism of attraction is that a Wigner crystal on one macro-ion interlocks with the Wigner crystal on another macro-ion, so that the positive charges associated with one macro-ion lie close to the negative regions on the other and visa versa [6,26]. Correlation effects are driven by two main factors: surface charge density and valance of counter-ions. As both of these increases, the stronger correlations are expected to become. In determining correlation effects, both the size and shape of the macro-ion are likely to have an important role. For instance, a flat, infinite charged surface has a proper Wigner crystal phase; but a charged rod may not or may have, depending on its radius. This is owing to the quasi-one dimensional nature of a cylindrical macro-ion surface [1], which makes thermal fluctuations at the macro-ion surface, which disrupt such a lattice, much larger.

In a lot of cases, most notably DNA, it may not be sufficient to think of macro-ions as uniformly charged [1,27]. It has been shown that structure of helical macro-ions, and of counter-ions bound to their surfaces, may cause attraction between them [1,12,21]. This mechanism of attraction is most pronounced when ions are able to bind strongly in helical motifs that lie between the helical patterns fixed charged groups, on the surface of the macro-ion, creating an alternating pattern of charge [1]. In the case of DNA, there is strong evidence to suggest that such localized binding, due to chemi-adsorption, does occur. For instance, evidence suggests this to be the case for polyamines [1,28,29] and Mn^{2+} [1,30,31], as counter-ions. As in the case of the Wigner crystal, the mechanism of attraction lies in fact that bound positive charges on one molecule lie close to the negative charges of the other molecule in a commensurate interlocking fashion; an electrostatic zipper [21]. In addition, how the shape of the charge distribution influences the interaction should be important in understanding the formation of cholesteric phases [32,33] and in the statistical mechanics of columnar macro-molecular assemblies [34,35]. Also, there may be reverse interplay between the structure of certain macro-ions and their interactions; the latter may indeed, sometimes, influence the former [1,36,37,38]. Sill, the parameters that describe the effective charge distributions on helical molecules (KL parameters) [1] have not been calculated from any microscopic theory.

Image charge effects and solvent effects should not be ignored. It seems reasonable to assume that the core of a macro-ion should have a much smaller dielectric response than a surrounding polar solvent [39]. This situation can create repulsive effects due to charges effectively seeing image charge reflections of themselves in regions of low dielectric constant. Even for the interaction between two uniformly charged rods, this can give rise to a new contribution to the interaction potential [12]. This repulsive interaction has half the range of standard screened electrostatic interaction. It arises from the charges on one molecule experiencing the force due image charges of themselves on the other molecule. Beyond the Poisson Boltzmann equation image charge effects in the interaction of individual small ions with macro-ion become important [5,10]. Here, the effects could be quite subtle. Image charge effects may increase the threshold at which correlation effects cause attraction, in terms of surface charge density and ionic valance [5]; but, in certain cases, they may cause increased attraction [10]. Other important effects could arise from the discreteness of the solvent. This can yield a non-local and non-linear dielectric response [15,16,17,18] and cause hydration forces between macro-ions [12,14,40]. Also,

one should also point out that image charge effects on solvent molecules could have an important role in determining cylinder-cylinder interactions, at small separations [41,42].

In addition, the finite size of the small ions may have a role in controlling the size of both image charge and correlation effects. As has already been pointed out, in [1]; the finite size of charge distributions of certain counter ions may significantly reduce correlation effects. The saturation of the local density of ions close to surface of macro-ions [43] should, also, be considered.

One way of handling some of these effects, in a systematic way, is to reformulate the statistical mechanical model that describes the macro-ion electrolyte system into a statistical field theory [3,43,44]. The advantage in such a formulation is that mean field of the fluctuating field used in such a theory is the thermally averaged electrostatic field. This allows for electrostatic boundary conditions due to the macro-ion solvent interface to be handled in a convenient manner. Another possible advantage is that statistical field theories have many levels of self-consistent approximation, most notable of which are the Hartree approximation and random phase approximations. These self consistent approximations may be built up in a systematic manner. Such self-consistent approximations have enjoyed notable success in other areas of condensed matter physics, and may yet provide new useful line of attack in understanding polyelectrolyte interactions. These particular field theories, which arise from such models, enjoy another important advantage: one can do a strong coupling expansion [3,5,10]. Such an expansion is valid when the ions in solution are highly correlated.

Our goal is to follow on from previous work in a series of papers, developing this field theoretic formulation. We hope to include the effects of finite size, image charge effects, chemi-adsorption, structure of charged groups, and perhaps, later, model the solvent in a more sophisticated way. Though, incorporating the last of these ingredients into the theory is probably the hardest. In this first paper, we start with a single macro ion in considering some of these effects. We show how chemi-adsorption, the finite size charge distribution of the small ions and interface effects between the macro-ion and the solvent solution may all be included in a field theoretic formulation. We then go on to approximate solutions to equations derived from this formalism for the simplest case of a uniformly charged rod.

In Section 2 we start by discussing the statistical mechanical model we shall use. Here, we show how quantities like the average electric field due to the ions and fixed charges, as well as the effective interaction (fluctuating potential) between two (infinitesimal) test charges in solution may be calculated from the partition function. We also discuss how the more traditional Kirkwood hierarchy [8] is obtained from the model.

Next we briefly describe how such a model may be transformed into a field theory; the details being left to one of the appendices. This is followed a description of the resulting theory. We also *prove* both that the average electrostatic potential is the mean field of the fluctuating field of such a theory, also that the correlation function of the fluctuating field is proportional to the effective interaction between the two test charges. All of this is considered in Section 3.

In Section 4, we describe the Gaussian (saddle-point) approximation of such a field theory. We show that the mean field satisfies the PB equation. Also we show the form of the free energy, which is not much different from that of [44]. Furthermore, we are able to recast it in a more conventional form [8] and are so able discuss the physics of each

term. In the next section (Section 5) we move on to consider the Hartree approximation to our field theory. This takes the form of two coupled equations, not too dissimilar to those derived by the authors of [44] in their most sophisticated variational approximation. This approximation [44] is, in fact, a Hartree approximation. Of the derived equations, one is a modified PB for average electrostatic field, the other an equation for the correlation function. In Section 6 we are able to extend our formalism to describe extended ionic charges and derive generalized Hartree equations, for this case. This completes the formal development.

In Section 7 we solve these equations for the uniformly charged rod, without chemi-adsorption, employing a WKB like approximation to handle the equation for the correlation function. This simplifying approximation is described in the previous two sections. This is similar to the approach used in [13], however this is employed for cylindrical geometry and goes beyond the Gaussian level of approximation. In our calculations we consider only spherically symmetric charge distributions and univalent ions. We present results for the average potential, charge density, and a function $\lambda(\mathbf{r})$ that describes the relative strength of image and correlation effects on individual ions. Also, we see how all of this fits into the framework of an effective theory of interaction of two charged cylinders with image charge effects [12], and calculate the effective charge compensation parameter θ. Last of all we estimate the quantitative accuracy of this WKB like approximation to the exact Hartree solution, by calculating a first order correction.

Last of all we have discussion (Section 8) and a conclusion and outlook (Section 9), where we summarize our findings and discuss the extensions that we hope to address in future work.

2. The statistical mechanical model

2.1 Description of model

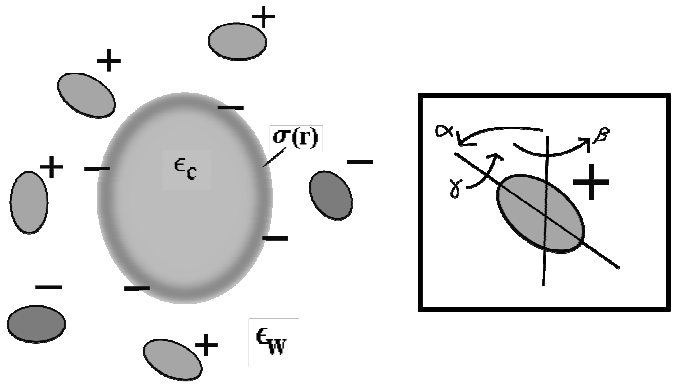

Fig.1 Schematic picture of the macro-ion-electrolyte system. In the box is shown how the orientation of an ion is described through Euler angles $\boldsymbol{\omega} = (\alpha, \beta, \gamma)$.

Let us consider a statistical mechanical model of a single large cylindrical macro-ion sitting in a 1:1 electrolyte solution. Let us assume that core region of the macro-ion may

be described by a region of low dielectric constant ($\varepsilon_c \approx 2$), whereas we will consider the solvent as a medium of high dielectric constant ($\varepsilon_w \approx 80$). The counter-ions (and electrolyte ions) are restricted to the solvent, which indeed envelops the macro-ion. We suppose that there are only two species of small ion in the solution. We center the macro-ion at the origin of a cylindrical coordinate system (z, R, φ) so that its major axis lies at $R = 0$. We start by considering the ionic charge distributions of the small ions to be of arbitrary shape. A schematic picture of a system is shown in Fig.1. Extending upon Ref [44], we may write down a partition function to describe a system containing these two regions of dielectric constant. This may be expressed as a functional of ionic density functions

$$Z[\hat{\rho}_+(\mathbf{r}), \hat{\rho}_-(\mathbf{r})] = \frac{1}{N_+!}\prod_{j=1}^{N_+}\int \frac{d^3 r_j^+}{\lambda_t^3}\int \frac{d^3\omega_j^+}{8\pi^2}\frac{1}{N_-!}\prod_{j=1}^{N_-}\int \frac{d^3 r_j^-}{\lambda_t^3}\int \frac{d^3\omega_j^-}{8\pi^2}\Omega_I\left(\mathbf{r}_j^+, \boldsymbol{\omega}_j\right)\Omega_I\left(\mathbf{r}_j^-, \boldsymbol{\omega}_j\right)$$
$$\times \exp\left(-\frac{\tilde{E}_{\text{int}}\{\mathbf{r}_j, \boldsymbol{\omega}_j\}}{k_B T}\right)\exp\left(-\frac{\tilde{E}_{self}\{\mathbf{r}_j, \boldsymbol{\omega}_j\}}{k_B T}\right), \tag{2.1}$$

where λ_t is the thermal de-Broglie wavelength. Here N_+ and N_- are the numbers of small positive and small negative ions, respectively, in the solution. The vectors $\mathbf{r}_j^-$ and $\mathbf{r}_j^+$ describe the positions of negative and positive ions respectively. The vectors $\boldsymbol{\omega}_j^-$ and $\boldsymbol{\omega}_j^+$ describe the orientation of each ion and have the three Euler angles (α, β, γ) as their components. The density functions are defined as $\hat{\rho}_+(\mathbf{r}) = \sum_{j=1}^{N_+} f_+(\mathbf{r} - \mathbf{r}_j^+, \boldsymbol{\omega}_j)$ and $\hat{\rho}_-(\mathbf{r}) = \sum_{j=1}^{N_-} f_-(\mathbf{r} - \mathbf{r}_j^-, \boldsymbol{\omega}_j)$, for positive and negative ions respectively. The form factors, f_+ and f_- describe extended distributions of charge on each ion, and are normalized so that $\int d^3 r\, f(\mathbf{r}, \boldsymbol{\omega}) = 1$. In the limit of point like charges, we take $f_+(\mathbf{r} - \mathbf{r}', \boldsymbol{\omega}) = f_-(\mathbf{r} - \mathbf{r}', \boldsymbol{\omega}) = \delta(\mathbf{r} - \mathbf{r}')$. Here, $\Omega_I\left(\mathbf{r}, \boldsymbol{\omega}\right)$ is termed the ionic exclusion function. This function is to insure that there is no Boltzmann weight given to the unphysical situation of an ion lying within the core region. If we consider the shape of our small ions as spherical, for a single cylindrical polyelectrolyte of radius a centered at the origin it simply takes the form: $\Omega_I\left(\mathbf{r}, \boldsymbol{\omega}\right) = \theta(R - b)$, where $b \geq a$. This inequality accounts for a hardcore radius of each ion. The hardcore radius may be taken to be the radius of the ion together with its inner hydration shell, which is tightly bound to the ion.

The total interaction energy between ions $\tilde{E}_{\text{int}} / k_B T$ takes the form (as in [44] with point charges)

$$\frac{\tilde{E}_{\text{int}}\{\mathbf{r}_j,\boldsymbol{\omega}_j\}}{k_BT}=\frac{l_B}{2}\int d\mathbf{r}\int d\mathbf{r}'\left[q\hat{\rho}_+(\mathbf{r})-q\hat{\rho}_-(\mathbf{r})+\sigma(\mathbf{r})\right]v(\mathbf{r},\mathbf{r}')\left[q\hat{\rho}_+(\mathbf{r}')-q\hat{\rho}_-(\mathbf{r}')+\sigma(\mathbf{r}')\right]$$
$$-\frac{q^2l_B}{2}\sum_j\int d^3r\int d^3r' f_-(\mathbf{r}-\mathbf{r}_j^-,\boldsymbol{\omega}_j)v(\mathbf{r},\mathbf{r}')\,f_-(\mathbf{r}'-\mathbf{r}_j^-,\boldsymbol{\omega}_j)+f_+(\mathbf{r}-\mathbf{r}_j^+,\boldsymbol{\omega}_j)v(\mathbf{r},\mathbf{r}')\,f_+(\mathbf{r}'-\mathbf{r}_j^+,\boldsymbol{\omega}_j),$$

(2.2)

where $l_B=e^2/(4\pi\varepsilon_w k_BT)$ is Bjerrum length and $\sigma(\mathbf{r})$ is the charge density of fixed charge groups that lie on the macro-ion. The valance of each ion is denoted by the integer q. Since we are only considering a 1:1 electrolyte both the negative and positive ions have been taken to have the same valance, though the model can be generalized for arbitrary valances. The function $eqv(\mathbf{r},\mathbf{r}')/4\pi\varepsilon_w$ is the electrostatic potential at the point $\mathbf{r}$ due to an ion centered at $\mathbf{r}'$, with which the other ions in the system interact. Now, the dielectric boundary, between the solvent and core regions, distorts the electrostatic potential of the ion: it does not take the form of a simple $1/r$ coulomb potential. Instead, it must satisfy the following Poisson equation:

$$\chi(\mathbf{r})\nabla^2 v(\mathbf{r},\mathbf{r}')=4\pi\delta(\mathbf{r}-\mathbf{r}'),\tag{2.3}$$

where for a cylindrical macro-ion

$$\chi(\mathbf{r})=\left[\theta(a-R)\frac{\varepsilon_c}{\varepsilon_w}+\theta(R-a)\right].\tag{2.4}$$

The usual electrostatic boundary conditions, the continuity of potential and the continuity of the component of the displacement field, $\mathbf{D}$ normal to the dielectric interface, apply at the macro-ion surface. Mathematically, these boundary conditions arise naturally from proper inversion of the operator $\chi(\mathbf{r})\nabla^2$ to find $v(\mathbf{r},\mathbf{r}')$. For the moment, we do not actually need to solve this equation for the single ion to make progress.

Now, because of an interface, we now have a new term in the partition function

$$\frac{\tilde{E}_{self}\{\mathbf{r}_j,\boldsymbol{\omega}_j\}}{k_BT}=\frac{1}{k_BT}\int d\mathbf{r}\int d\mathbf{r}'\hat{\rho}_+(\mathbf{r})v_c(\mathbf{r}-\mathbf{r}')\gamma(\mathbf{r}')$$
$$\frac{q^2l_B}{2}\sum_j\int d^3r\int d^3r'\left[f_-(\mathbf{r}-\mathbf{r}_j^-,\boldsymbol{\omega}_j^-)v(\mathbf{r},\mathbf{r}')\,f_-(\mathbf{r}'-\mathbf{r}_j^-,\boldsymbol{\omega}_j^-)-\lim_{r_j^+\to\infty}f_-(\mathbf{r}-\mathbf{r}_j^-,\boldsymbol{\omega}_j^-)v(\mathbf{r},\mathbf{r}')\,f_-(\mathbf{r}'-\mathbf{r}_j^-,\boldsymbol{\omega}_j^-)\right]$$
$$+\frac{q^2l_B}{2}\sum_j\int d^3r\int d^3r'\left[f_+(\mathbf{r}-\mathbf{r}_j^+,\boldsymbol{\omega}_j^+)v(\mathbf{r},\mathbf{r}')\,f_+(\mathbf{r}'-\mathbf{r}_j^-,\boldsymbol{\omega}_j^+)-\lim_{r_j^+\to\infty}f_+(\mathbf{r}-\mathbf{r}_j^+,\boldsymbol{\omega}_j^+)v(\mathbf{r},\mathbf{r}')\,f_+(\mathbf{r}'-\mathbf{r}_j^+,\boldsymbol{\omega}_j^+)\right]$$

(2.5)

This term is the sum of the changes in the self energy of each ion, moving from the bulk ($\mathbf{r} \to \infty$) to a position in the vicinity of the polyelectrolyte, $\mathbf{r}_j$. It is comprised of two contributions. The last two terms (on the RHS of Eq. (2.5)) are the change in electrostatic self energy. As all ions experience increased repulsion as they move towards the region of low dielectric, this term is positive. It depends on the position of each ion; therefore it must be included in the partition function to adequately describe the system. Each term in the sum (of Eq. (2.5)) may be thought of as a change in hydration energy of a single ion. The first term in Eq. (2.5) represents the change in energy due to chemi-adsorption close to the surface of the macro-ion. Here, $v_c(\mathbf{r}-\mathbf{r}')$ is the chemi- adsorption potential due to one particular chemical group on the macro-ion and $\gamma(\mathbf{r}')$ is the density of such groups. In writing Eq.(2.5), we have supposed that only the positive ions feel such a potential, but one can simply modify the theory to take account of chemi-adsorption of negative ions.

2.2 Mean potential and fluctuation potential.

In such a model we may introduce two test charges q_1 and q_2 lying at the points $\mathbf{r}_1$ and $\mathbf{r}_2$, respectively. We may define $\tilde{E}_{\text{int}}\{\mathbf{r}_j, \boldsymbol{\omega}_j\}(q_1, q_2)$, where we replace $\sigma(\mathbf{r})$ with $\sigma(\mathbf{r}) + q_1\delta(\mathbf{r}-\mathbf{r}_1) + q_2\delta(\mathbf{r}-\mathbf{r}_2)$ in (2.2). These two test charges allow us to calculate two physical quantities

$$\phi_0(\mathbf{r}_1) = -\lim_{\substack{q_1\to 0\\ q_2\to 0}}\left[\frac{k_B T}{e}\frac{\partial}{\partial q_1}\ln Z(q_1,q_2)\right] \quad \text{and} \quad W(\mathbf{r}_1,\mathbf{r}_2) = -\lim_{\substack{q_1\to 0\\ q_2\to 0}}\left[k_B T\frac{\partial^2}{\partial q_1 \partial q_2}\ln Z(q_1,q_2)\right], \tag{2.6}$$

where $Z(q_1, q_2)$ denotes the partition function with the two test charges included. In these definitions, the positions of the test charges are not integrated over. Instead, these charges are taken infinitesimally small so as not to disturb the many-body system. As we will see below, the first of these two expressions is indeed the average potential a test charge experiences from the ions and the fixed charges. Whereas, $q_1 q_2 W$ is the average interaction energy between the two test charges.

Using Eq. (2.1) and (2.2) in Eq. (2.6), we may derive the following expressions for ϕ_0 and W.

$$\phi_0(\mathbf{r}_1) = \frac{e}{4\pi\varepsilon_w}\int d^3r' v(\mathbf{r}_1,\mathbf{r}')\left\langle q\rho(\mathbf{r}') - q\rho(\mathbf{r}') + \sigma(\mathbf{r}')\right\rangle \ , \tag{2.7}$$

and

$$W(\mathbf{r}_1,\mathbf{r}_2)=\frac{e^2 v(\mathbf{r}_1,\mathbf{r}_2)}{4\pi\varepsilon_w}-\frac{e^2 l_B}{4\pi\varepsilon_w}\int d^3r\int d^3r' v(\mathbf{r}_1,\mathbf{r})v(\mathbf{r}_2,\mathbf{r}')\Big[\big\langle[q\hat{\rho}_+(\mathbf{r})-q\hat{\rho}_-(\mathbf{r})][q\hat{\rho}_+(\mathbf{r}')-q\hat{\rho}_-(\mathbf{r}')]\big\rangle$$
$$-\big\langle[q\hat{\rho}_+(\mathbf{r})-q\hat{\rho}_-(\mathbf{r})]\big\rangle\big\langle[q\hat{\rho}_+(\mathbf{r}')-q\hat{\rho}_-(\mathbf{r}')]\big\rangle\Big]. \tag{2.8}$$

Here, $\langle\ldots\rangle$ denotes statistical averaging over all the degrees of freedom associated with the position and orientation of the ions. In Eq. (2.7) $\int d^3r' v(\mathbf{r}_1,\mathbf{r}')(q\rho_+(\mathbf{r}')-q\rho_-(\mathbf{r}')+\sigma(\mathbf{r}'))$ is simply the solution of Poisson's equation for each configuration of the ions, which is averaged with the appropriate Boltzmann weight. Therefore, the function $\phi_0(\mathbf{r}_1)$ is, indeed, the *mean electrostatic potential of the system*.

For Eq. (2.8) there are two terms. The first term represents the bare electrostatic interaction between the two test charges. The second term is a renormalization of the interaction arising from the movement of the ions to screen out the interaction. We call this a fluctuating potential. However, this fluctuating potential is quite different from the one given in Ref. [8]. This latter is defined for point charges, which we denote by $\phi_f(q,\mathbf{r},\mathbf{r}')$. The formula for $\phi_f(q,\mathbf{r},\mathbf{r}')$ may be found by considering the average density function $c(\mathbf{r})=\big\langle[\hat{\rho}_+(\mathbf{r}_1)+\hat{\rho}_-(\mathbf{r}_1)]\big\rangle$, averaged using $\tilde{E}_{\text{int}}\{\mathbf{r}_j\}(q_1,0)$, where the position of the point charge q_1 is now averaged over and is taken to be finite. The trick is, when $q_1\to q$, it becomes indistinguishable from any small point like positive ion in the electrolyte solution.

Then, one may show that

$$\frac{\partial\ln c(\mathbf{r})}{\partial q_1}=\frac{\partial\ln Z}{\partial q_1}-l_B\int d^3r' v(\mathbf{r}_1,\mathbf{r}')\frac{\big\langle[q\rho(\mathbf{r}')-q\rho(\mathbf{r}')+q_1\delta(\mathbf{r}_1-\mathbf{r}')+\sigma(\mathbf{r}')][\hat{\rho}_+(\mathbf{r}_1)+\hat{\rho}_-(\mathbf{r}_1)]\big\rangle}{\big\langle[\hat{\rho}_+(\mathbf{r}_1)+\hat{\rho}_-(\mathbf{r}_1)]\big\rangle}. \tag{2.9}$$

It is possible to get rid of $\frac{\partial\ln Z}{\partial q_1}$ by subtracting away the bulk concentration $c_b=\lim_{r_1\to\infty}\big\langle[\hat{\rho}_+(\mathbf{r}_1)+\hat{\rho}_-(\mathbf{r}_1)]\big\rangle$. In such a way it is possible to show that

$$\frac{k_BT}{e}\frac{\partial}{\partial q_1}\ln\left[\frac{c(\mathbf{r})}{c_b}\right]=\phi_0(q_1;\mathbf{r})+\phi_f(q_1;\mathbf{r},\mathbf{r})-\lim_{r\to\infty}\phi_f(q_1;\mathbf{r},\mathbf{r}) \tag{2.10}$$

where the fluctuating potential is given by

$$\phi_f(q_1;\mathbf{r},\mathbf{r}')=\frac{e}{4\pi\varepsilon_w}\int d^3r'' v(\mathbf{r},\mathbf{r}'')\left[\frac{\big\langle[q\rho(\mathbf{r}'')-q\rho(\mathbf{r}'')+q_1\delta(\mathbf{r}-\mathbf{r}'')][\hat{\rho}_+(\mathbf{r}')+\hat{\rho}_-(\mathbf{r}')]\big\rangle}{\big\langle[\hat{\rho}_+(\mathbf{r}')+\hat{\rho}_-(\mathbf{r}')]\big\rangle}-\big\langle[q\rho(\mathbf{r}'')-q\rho(\mathbf{r}'')]\big\rangle\right] \tag{2.11}$$

Both Eqs. (2.7) and (2.11) form the starting basis of a hierarchy of equations known as the Kirkwood hierarchy [45]. Evaluation of the concentration is performed by charging the charge, q_1 from 0 up q, through integration of Eq. (2.10) with respect to q_1. Higher order equations in the hierarchy may be got by performing successive differentiations in q_1 on the average number density. Using both Eqs. (2.11) and (2.8) ,one may relate both fluctuating potentials to one another

$$W(\mathbf{r}_1,\mathbf{r}_2) = l_B \int d^3r' v(\mathbf{r}_1,\mathbf{r}') \langle \rho(\mathbf{r}') \rangle \phi_f(0;\mathbf{r}',\mathbf{r}_2) + \frac{e}{4\pi\varepsilon_w} v(\mathbf{r}_1,\mathbf{r}_2). \tag{2.12}$$

But, as we shall in the next, the correlation function $W(\mathbf{r}_1,\mathbf{r}_2)$ is much more convenient for considering correlations in a field theoretical formulation than $\phi_f(q;\mathbf{r},\mathbf{r}')$.

2.3 Grand canonical ensemble.

In what follows, instead of an ensemble of fixed particle number, it will be more convenient for us to consider the grand partition function, which takes the form;

$$Z_\lambda = \sum_{N_+,N_-=0}^{\infty} \left(\lambda^+\right)^{N_+} \left(\lambda^-\right)^{N_-} Z. \tag{2.13}$$

Here, λ^+ and λ^- are the positive and negative ion fugacities. These may be easily related to usual chemical potentials μ_+ and μ_- simply by $\lambda^+ = \exp\left(\mu_+ / k_B T\right)$ and $\lambda^- = \exp\left(\mu_- / k_B T\right)$, respectively. The average number of positive ion and negative ions are given by the following expressions

$$\langle N_+ \rangle = \frac{\partial \ln Z_\lambda}{\partial \lambda_+} \quad \text{and} \qquad \langle N_- \rangle = \frac{\partial \ln Z_\lambda}{\partial \lambda_-}. \tag{2.14}$$

As the macro-ion-electrolyte system is electrically neutral, we must have the condition that $q\langle N_+ \rangle + \int d^3r \sigma(\mathbf{r}) = q\langle N_- \rangle$. But, in the thermodynamic limit for an isolated macro-ion in electrolyte solution $\langle N_+ \rangle \to \infty$. Then, for point ions and both ions having the same shape, electro-neutrality can be achieved by simply setting the two fugacities equal $\lambda_+ = \lambda_- = \lambda$. In the next section we will be able to derive expressions for these quantities in the field theoretical formulation.

3. The field theoretical formulation for point like ions

Here we consider $f_+(\mathbf{r}-\mathbf{r}',\boldsymbol{\omega}) = f_-(\mathbf{r}-\mathbf{r}',\boldsymbol{\omega}) = \delta(\mathbf{r}-\mathbf{r}')$. Now, using a trick used in [44] we may start to transform this statistical mechanical model into a field theory, where we may write the following identity

$$Z[\hat{\rho}_+(\mathbf{r}),\hat{\rho}_-(\mathbf{r})] \equiv \int \mathfrak{D}\rho_+(\mathbf{r})\int \mathfrak{D}\rho_-(\mathbf{r})\delta^{\infty}(\hat{\rho}_+(\mathbf{r})-\rho_+(\mathbf{r}))\delta^{\infty}(\hat{\rho}_-(\mathbf{r})-\rho_-(\mathbf{r}))Z[\rho_+(\mathbf{r}),\rho_-(\mathbf{r})]$$
$$= \int \mathfrak{D}\rho_+(\mathbf{r})\int \mathfrak{D}\rho_-(\mathbf{r})\int \mathfrak{D}\psi_+(\mathbf{r})\int \mathfrak{D}\psi_-(\mathbf{r})\exp\left\{i\int d^3r\left[\psi_+(\mathbf{r})\left(\rho_+(\mathbf{r})-\hat{\rho}_+(\mathbf{r})\right)+\psi_-(\mathbf{r})\left(\rho_-(\mathbf{r})-\hat{\rho}_-(\mathbf{r})\right)\right]\right\}$$
$$\times Z[\rho_+(\mathbf{r}),\rho_-(\mathbf{r})]. \tag{3.1}$$

This reformulation (through Eq. (3.1)) has an immediate advantage when we come to consider the grand partition function, as we may use Eq, (3.1) to readily perform the sums in Eq.(2.13) (see Appendix A). As is shown in Appendix A and Ref. [44], it is possible to integrate out both $\rho_+(\mathbf{r})$ and $\rho_-(\mathbf{r})$ as well as one of the ψ-fields. We integrate out $\psi_+(\mathbf{r})$ and set $\psi_-(\mathbf{r}) = \phi(\mathbf{r})$ in doing so we arrive at the grand partition function being described by the following field theory

$$Z_\lambda = \frac{1}{Z_{VAC}}\int \mathfrak{D}\phi(\mathbf{r})\exp\left(-H_{ion}[\phi(\mathbf{r})]/\Xi\right), \tag{3.2}$$

where

$$H_{ion}[\phi(\mathbf{r})] = \int d^3r\left[\frac{1}{4}\chi(\mathbf{r})\left(\nabla\phi(\mathbf{r})\right)^2 + i\tilde{\sigma}(\mathbf{r})\phi(\mathbf{r}) - \frac{\tilde{\kappa}^2}{2\Lambda}\Omega(\mathbf{r})\cos\phi(\mathbf{r})\right.$$
$$\left. - \frac{\tilde{\kappa}^2}{4\Lambda}\Omega(\mathbf{r})e^{-i\phi(\mathbf{r})}\left(e^{-V_{ch}(\mathbf{r})}-1\right)\right] \tag{3.3}$$

We should point out that all lengths and positions $\mathbf{r}$ in Eq. (3.3) have been rescaled to measure in Gouy-Chapman lengths, so to match with the results of Ref. [44]. Such a unit length is given by $\mu = \dfrac{e}{2\pi q l_B \sigma_s}$. Also, in Eq. (3.3) , we have a rescaled charge density so that $\tilde{\sigma}(\mathbf{r}) = e\mu\sigma(\mathbf{r}\mu)/\sigma_s$. The effective surface charge density σ_s is given by

$$\sigma_s = e\int d^3r\sigma(\mathbf{r})/S_{\inf}\ , \tag{3.4}$$

and $S_{\inf}$ is the effective surface area of interface. One should note that Eq. (3.4) is expressed in normal units of length, not Guoy-Chapman lengths, as σ_s defines the Guoy-Chapman length. Also, we have a rescaled inverse Debye screening length $\tilde{\kappa} = \mu\kappa_D$. As

usual the Debye screening length for a 1:1 electrolyte is given by $\kappa_D^2 = 8\pi q^2 l_B n_{salt}$, where n_{salt} is the number concentration of ion pairs in solution. This is related to the recalled fugacity $\tilde{\lambda} = 2\lambda_R / \pi l_B \sigma_s^2$ and $\lambda_R = \lambda(q^2 l_B v(\infty,\infty)/2 - 3\ln\lambda_t)$, through the following relationship for a single macro-ion

$$\tilde{\kappa}^2 = \tilde{\lambda}\Lambda, \qquad \text{where} \qquad \Lambda = \lim_{\mathbf{r}\to\infty}\left\langle \exp i\phi(\mathbf{r})\right\rangle . \tag{3.5}$$

Eq. (3.5) is derived in Appendix A.

The last term on the RHS of Eq. (3.3) represents an imbalance of counter charges due to a chemi-adorbtion potential. The degree of this imbalance depends on the Boltzmann factor $\exp(-V_{ch}(\mathbf{r}))$, which is given by

$$V_{ch}(\mathbf{r}) = \frac{1}{k_B T}\int v_c(\mu\mathbf{r} - \mathbf{r}')\gamma(\mathbf{r}')d\mathbf{r}' . \tag{3.6}$$

What plays a crucial role in the theory described by Eqs. (3.2)-(3.6) is the correlation parameter

$$\Xi = \left(2\pi\right)^2 l_B^2 \sigma_s q^3 / e . \tag{3.7}$$

This is an important measure of the amount of correlations between ions, near the surface of the macro-ion. We will discuss its role more detail in the next section.

Included in Eq. (3.2) is

$$Z_{VAC} = \int D\phi(\mathbf{r}) \exp\left[-H_0[\phi(\mathbf{r})]/\Xi\right] \tag{3.8}$$

$$H_0[\phi(\mathbf{r})] = \int d^3 r\left[\frac{1}{4}\chi(\mathbf{r})\left(\nabla\phi(\mathbf{r})\right)^2\right]. \tag{3.9}$$

This factor insures that vacuum fluctuations ($\tilde{\kappa}\to 0$) in the field $\phi(\mathbf{r})$ are not considered, *the only fluctuations in* $\phi(\mathbf{r})$ *arise from movement of the ions*. In the field theoretical formulation we may evaluate both ϕ_0 and W for the grand canonical ensemble. We have that

$$\phi_0(\mathbf{r}_1) = -\lim_{\substack{q_1\to 0\\ q_2\to 0}}\left[\frac{k_B T}{e}\frac{\partial}{\partial q_1}\ln Z_\lambda(q_1,q_2)\right] \quad \text{and} \quad W(\mathbf{r}_1,\mathbf{r}_2) = -\lim_{\substack{q_1\to 0\\ q_2\to 0}}\left[k_B T\frac{\partial^2}{\partial q_1\partial q_2}\ln Z_\lambda(q_1,q_2)\right] \tag{3.10}$$

where now

$$Z_\lambda(q_1,q_2) = \frac{1}{Z_{VAC}}\int \mathfrak{D}\phi(\mathbf{r})\exp\left(-H_{ion}[\phi(\mathbf{r})]/\Xi - i\frac{q_1}{q}\phi(\mathbf{r}_1) - i\frac{q_2}{q}\phi(\mathbf{r}_2)\right). \tag{3.11}$$

Evaluating both expressions yields the following relationships

$$\phi_0(\mathbf{r}_1) = \frac{ik_B T}{qe}\langle\phi(\mathbf{r}_1)\rangle \quad \text{and}$$

$$W(\mathbf{r}_1,\mathbf{r}_2) \equiv \frac{k_B T}{q^2}\left[\langle\phi(\mathbf{r}_1)\phi(\mathbf{r}_2)\rangle - \langle\phi(\mathbf{r}_1)\rangle\langle\phi(\mathbf{r}_2)\rangle\right] = \frac{k_B T\Xi V(\mathbf{r}_1,\mathbf{r}_2)}{q^2}\ . \tag{3.12}$$

Therefore, we are able assign physical meaning to both the mean field and the two point correlation function of the field theory.

4. Gaussian approximation

Here we evaluate the mean field in the Gaussian approximation. We may write $\phi(\mathbf{r}) = \phi'(\mathbf{r}) - i\phi_0(\mathbf{r})$ with $\phi_0(\mathbf{r}) = i\langle\phi(\mathbf{r})\rangle$. Then we may expand out in powers of the fluctuating field $\phi'(\mathbf{r})$. At the lowest order of approximation (the Gaussian) we obtain

$$Z_\lambda \approx \frac{\exp\left((-E_0[\phi_0(\mathbf{r})] + \Lambda_0\Delta E[\phi_0(\mathbf{r})])/\Xi\right)}{Z_{VAC}}\int \mathfrak{D}\phi'(\mathbf{r})\exp\left(-H_G[\phi(\mathbf{r})]/\Xi\right), \tag{4.1}$$

where

$$E_0[\phi_0(\mathbf{r})] = \int d^3r\left[-\frac{1}{4}\chi(\mathbf{r})\left(\nabla\phi_0(\mathbf{r})\right)^2 + \tilde{\sigma}(\mathbf{r})\phi_0(\mathbf{r}) - \frac{\tilde{\kappa}^2}{2}\Omega_I(\mathbf{r})\cosh\phi_0(\mathbf{r})\right.$$
$$\left. - \frac{\tilde{\kappa}^2}{4}\Omega_I(\mathbf{r})e^{-\phi_0(\mathbf{r})}\left(e^{-V_{ch}(\mathbf{r})} - 1\right)\right], \tag{4.2}$$

$$\Delta E[\phi_0(\mathbf{r})] = \int d^3r \left[\frac{\tilde{\kappa}^2}{2} \Omega_I(\mathbf{r}) \cosh \phi_0(\mathbf{r}) + \frac{\tilde{\kappa}^2}{4} \Omega_I(\mathbf{r}) e^{-\phi_0(\mathbf{r})} \left(e^{-V_{ch}(\mathbf{r})} - 1 \right) \right] , \tag{4.3}$$

$$H_G[\phi_0(\mathbf{r})] = \int d^3r \left[\frac{1}{4} \chi(\mathbf{r}) \left(\nabla \phi'(\mathbf{r}) \right)^2 + \frac{\tilde{\kappa}^2}{4} \Omega_I(\mathbf{r}) \phi'(\mathbf{r})^2 \cosh \phi_0(\mathbf{r}) \right.$$
$$\left. - \frac{\tilde{\kappa}^2}{4} \Omega_I(\mathbf{r}) \phi'(\mathbf{r})^2 e^{-\phi_0'(\mathbf{r})} \left(e^{-V_{ch}(\mathbf{r})} - 1 \right) \right], \tag{4.4}$$

and $\Lambda_0 = 1/2 \lim_{r \to \infty} \left\langle \phi'(\mathbf{r})^2 \right\rangle$. The mean field must satisfy the condition $\delta E_0[\phi_0(\mathbf{r})] / \delta \phi_0(\mathbf{r}) = 0$, because we require that $\left\langle \phi'(\mathbf{r}) \right\rangle = 0$. This yields

$$\chi(\mathbf{r}) \nabla^2 \phi_0(\mathbf{r}) - \kappa^2 \Omega(\mathbf{r}) \sinh(\phi_0(\mathbf{r})) - e^{-\phi_0'(\mathbf{r})} \frac{\kappa^2 \Omega_C(\mathbf{r})}{2} \left(e^{-V_{ch}(\mathbf{r})} - 1 \right) = -2\sigma(\mathbf{r}) . \tag{4.5}$$

This is simply the non-linear P-B equation with an additional term to take account of chemi-adsorption. The free energy is given by

$$F = \frac{k_B T}{\Xi} E_0[\phi_0(\mathbf{r})] - \frac{\Lambda_0 k_B T}{\Xi} \Delta E[\phi_0(\mathbf{r})] - k_B T \ln \int \mathfrak{D} \phi'(\mathbf{r}) \exp\left(-H_G[\phi(\mathbf{r})] / \Xi \right) + \ln Z_{VAC} . \tag{4.6}$$

The sum of the last three terms may be considered as the leading order contribution due correlation effects. This free energy (Eq. (4.6)) has been considered for the case of two charged plates [10,13]. This result is the same as the one given in [44] (for the simpler variational principle of a renormalized charge density, see therein) when there is no chemi-adsorption, no dielectric boundary (i.e setting $\varepsilon_w = \varepsilon_c$), allowing ions to penetrate into the macro-ion, and replacing $\cosh \phi_0(\mathbf{r})$ by 1 in both Eq. (4.3) and Eq. (4.4) Following this prescription we indeed recover the expression given by (31) of [44], by rewriting Eq. (4.5)

$$\nabla^2 \phi_0(\mathbf{r}) = -\tilde{\sigma}(\mathbf{r}) - \tilde{\sigma}_C(\mathbf{r}) = -2\eta(\mathbf{r}) \tilde{\sigma}(\mathbf{r}) - \kappa^2 \phi_0(\mathbf{r}) . \tag{4.7}$$

In the limit of no correlations $\Xi \to 0$ the last two terms may be neglected in (4.6). By correctly identifying entropic and electrostatic energy components, it is possible free energy, in the limit $\Xi \to 0$, can be rewritten in a more conventional form [8]

$$F=\frac{e^2}{2}\int d^3r\phi(\mathbf{r})\left[\rho_+(\mathbf{r})-\rho_-(\mathbf{r})+\sigma(\mathbf{r})\right]-k_BT\int d^3r\left[\rho_+(\mathbf{r})\ln\rho_+(\mathbf{r})+\rho_-(\mathbf{r})\ln\rho_-(\mathbf{r})\right]$$
$$+k_BT\int d^3r\left[\rho_+(\mathbf{r})+\rho_-(\mathbf{r})\right] \tag{4.8}$$

where $\rho_+(\mathbf{r})$ and $\rho_-(\mathbf{r})$ are the number densities of positive and negative ions, respectively.

The first term in Eq. (4.8) is the electrostatic part and the second term is the contribution from the entropies of positive and negative ions. Here the last term in Eq. (4.8) is the contribution from entropy of the solvent for an ideal solution

$$S_{solv}=-\frac{k_B}{V_{ion}}\int d^3r\left[1-V_{ion}(\rho_+(\mathbf{r})+\rho_-(\mathbf{r}))\right]\ln\left(1-V_{ion}(\rho_+(\mathbf{r})+\rho_-(\mathbf{r}))\right), \tag{4.9}$$

expanded out for small $\rho_+(\mathbf{r})$ and $\rho_-(\mathbf{r})$. If we choose not to expand $\rho_+(\mathbf{r})$ and $\rho_+(\mathbf{r})$ in Eq. (4.9) and minimize the resulting free energy with respect to $\rho_+(\mathbf{r})$ and $\rho_-(\mathbf{r})$, subject to Poisson's equation $\nabla^2\phi(\mathbf{r})=-e\left[q\rho_+(\mathbf{r})-q\rho_-(\mathbf{r})+\sigma(\mathbf{r})\right]$, we arrive at equations for finite size ions effects discussed in Ref. [43].

We may ask what is the physical meaning of the last two terms in Eq (4.6). First, one is able to show that

$$\tilde{F}\equiv\ln\int\mathcal{D}\phi'(\mathbf{r})\exp\left(-H_G[\phi]/\Xi\right)-\ln Z_{VAC}=-\frac{1}{2\Xi}\int_0^{\tilde{\kappa}^2}d\tilde{\kappa}'^2\int d^3r\cos\phi_0(\mathbf{r})\left\langle\phi'(\mathbf{r})^2\right\rangle$$
$$=-\int_0^{c_{salt}}dc\int d^3r\left(\rho_+(\mathbf{r};c)/c+\rho_-(\mathbf{r};c)/c\right)W(\mathbf{r},\mathbf{r};c). \tag{4.10}$$

Here the concentration c_{salt} is defined by $c_{salt}=\tilde{\kappa}^2$. The physical meaning of this term is quite clear if we consider a small change from a bulk concentration c_{salt} to a concentration $c_{salt}+\Delta c_{salt}$

$$\Delta\tilde{F}=-\frac{\Delta c_{salt}}{c_{salt}}\int d^3r\left(\rho_+(\mathbf{r};c_{salt})+\rho_-(\mathbf{r};c_{salt})\right)W(\mathbf{r},\mathbf{r};c_{salt}). \tag{4.11}$$

It is easy to interpret this term as the sum of self-energies or change in solvation energy of each of the ions when changing the concentration by an infinitesimal amount. This is indeed, simply, the self energy of each ion $W(\mathbf{r},\mathbf{r};c_{salt})$ integrated with the change in the local electrolyte density $\frac{\Delta c_{salt}}{c_{salt}}\left(\rho_+(\mathbf{r};c_{salt})+\rho_-(\mathbf{r};c_{salt})\right)$. Since both the number densities and self-energies change must change with concentration, to calculate the self energy

contribution from all the ions to the free energy one must consider Eq. (4.10). Whereas, the change in the solvation energy of a single ion going from a region with salt concentration c'_{salt} to c_{salt} would be simply $W(\mathbf{r},\mathbf{r};c'_{salt})-W(\mathbf{r},\mathbf{r};c_{salt})$, provided that this does not effect the concentration of the two regions. The term proportional to Λ_0 simply removes a divergence in Eq. (4.11) due to the point like nature of the ions.

Thus, we see that the field theoretical formulation correctly describes the physics at this level of approximation. But, the Gaussian approximation is only valid provided that $\tilde{\kappa}$ and Ξ remain small. A perturbation theory may be developed for corrections to the PB in powers of Ξ. But, to consider larger values of Ξ it is possible to use a self-consistent approximation. We do so next section.

5. The Hartree approximation

We now go beyond the Gaussian approximation to include counter-ion correlation effects. We do this as in [44], and construct a variational trail energy functional, describing the fluctuating part of the field, of the form

$$H_H[\phi'(\mathbf{r})]=\int d^3r\phi'(\mathbf{r})V_H(\mathbf{r},\mathbf{r}')\phi'(\mathbf{r}'). \tag{5.1}$$

We then may expand the partition function about

$$Z_H[\phi'(\mathbf{r})]=\int \mathfrak{D}\phi \exp(-H_H[\phi'(\mathbf{r})]/\Xi), \tag{5.2}$$

to first order in $H_{ion}[\phi(\mathbf{r})]-H_H[\phi'(\mathbf{r})]$. Then have the following expression for the free energy

$$f_H=F_H/k_BT=-\ln Z_H+\left\langle H_{ion}[\phi(\mathbf{r})]-H_H[\phi'(\mathbf{r})]\right\rangle_H. \tag{5.3}$$

The subscript H on the averaging bracket denotes averaging with the Boltzmann weight $\exp(-H_H[\phi'(\mathbf{r})]/\Xi)$. On evaluation of the various terms Eq. (5.3) yields the following free energy

$$f_H=-\frac{1}{2}Tr\ln V_H(\mathbf{r},\mathbf{r}')-\frac{1}{\Xi}\int d^3r\left[\left\{\chi(\mathbf{r})\frac{\left(\nabla\phi_0(\mathbf{r})\right)^2}{4}+\sigma(\mathbf{r})\phi_0(\mathbf{r})+\frac{\tilde{\kappa}^2}{2}\Omega_I(\mathbf{r})\lambda(\mathbf{r})\cos\phi_0(\mathbf{r})\right\}\right]$$
$$+\frac{1}{4}\int d^3r\int d^3r'\delta(\mathbf{r}-\mathbf{r}')\chi(\mathbf{r})\nabla_{\mathbf{r}}\nabla_{\mathbf{r}'}V_H(\mathbf{r},\mathbf{r}')-\frac{1}{2}\int d^3r\int d^3r'\delta(0) \tag{5.4}$$

where

$$\lambda(\mathbf{r})=\exp\left(\Xi(V_H(\mathbf{r},\mathbf{r})-V_H(\infty,\infty))/2\right). \tag{5.5}$$

The quantity $\lambda(\mathbf{r})$ is essentially a Boltzmann weight associated with the change in the ionic self energy going from the Bulk to a position $\mathbf{r}$ near the Macro-ion.

We may use f_H to construct a variational principle as it satisfies the Gibbs - Bouglibogov inequality. This states that $f_H \geq f$, where f is the exact reduced free energy. For such a principle, we may treat $V_H(\mathbf{r},\mathbf{r}')$ and $\phi_0(\mathbf{r})$ as variational parameters to minimize the free energy i.e

$$\delta f_H / \delta V_H(\mathbf{r},\mathbf{r}') = 0 \quad \text{and} \quad \delta f_H / \delta \phi_0(\mathbf{r}) = 0 . \tag{5.6}$$

This yields the Hartree equations

$$\chi(\mathbf{r})\nabla^2\phi_0(\mathbf{r}) - \Omega_I(\mathbf{r})\tilde{\kappa}^2\lambda(\mathbf{r})\sinh\phi_0(\mathbf{r}) + \Omega_I(\mathbf{r})\frac{\tilde{\kappa}^2}{2}\lambda(\mathbf{r})\exp(-\phi_0(\mathbf{r}))\left(e^{-V_{ch}(\mathbf{r})}-1\right) = -2\tilde{\sigma}(\mathbf{r}) \tag{5.7}$$

$$\begin{aligned}&\chi(\mathbf{r})\nabla_{\mathbf{r}}^2 V_H(\mathbf{r},\mathbf{r}') - \Omega(\mathbf{r})\tilde{\kappa}^2\lambda(\mathbf{r})\cosh\phi_0(\mathbf{r})V_H(\mathbf{r},\mathbf{r}') \\ &-\Omega_I(\mathbf{r})\frac{\tilde{\kappa}^2}{2}\lambda(\mathbf{r})\exp(-\phi_0(\mathbf{r}))\left(e^{-V_{ch}(\mathbf{r})}-1\right)V_H(\mathbf{r},\mathbf{r}') = -2\delta(\mathbf{r}'-\mathbf{r})\end{aligned} \tag{5.8}$$

Such an approximation may be, indeed, be called a Hartree approximation, as these same equations may also be derived by diagrammatic expansion, where one sums over particular class of diagrams that correspond to such an approximation in field theory [46]. This diagrammatic derivation is shown in Appendix B (for $V_{ch} = 0$). Let us from now on we will consider $V_{ch} = 0$ [47].

If we set $\lambda(\mathbf{r}) = 1$ in Eq. (5.8), then $V_H(\mathbf{r},\mathbf{r}')$ obeys the same equation as $\phi_f(q,\mathbf{r}',\mathbf{r})$ in the linearized approximation described in [8]. In such an approximation one can show $\phi_f(q,\mathbf{r}',\mathbf{r})$ is linear in q. It is, then, not hard to show, under this prescription, both approximations yield the same Boltzmann weight $\lambda(\mathbf{r})$ and so the same modified PB equation. However, Eq. (5.8) with $\lambda(\mathbf{r}) \neq 1$ both formulations yield different equations. We suggest that the Hartree approximation may be more physically appropriate, as it depends self consistently on the local density of ions (see discussion at the end of the section), which may be shown to take the form $c(\mathbf{r}) = \Omega(\mathbf{r})\tilde{\kappa}^2\lambda(\mathbf{r})\cosh\phi_0(\mathbf{r})$.

In general we cannot obtain an analytical solution to Eq. (5.8) and the coupled equations are difficult to solve numerically as they stand. However in Appendix C, we are able to construct an approximate solution, which is used in the limit $\mathbf{r}' \to \mathbf{r}$. Instead of solving Eq. (5.8) we solve ($V_{ch} = 0$)

$$\chi(\mathbf{r})\nabla_{\mathbf{r}}^2\tilde{V}_H(\mathbf{r},\mathbf{r}') - \Omega(\mathbf{r})\tilde{\kappa}^2\lambda(\mathbf{r}')\cosh\phi_0(\mathbf{r}')\tilde{V}_H(\mathbf{r},\mathbf{r}') = -2\delta(\mathbf{r}'-\mathbf{r}) \tag{5.9}$$

We call this a WKB like approximation. In Appendix. C, we show how one may calculate the difference $\Delta V_H(\mathbf{r},\mathbf{r}') = V_H(\mathbf{r},\mathbf{r}') - \tilde{V}_H(\mathbf{r},\mathbf{r}')$ and so capture the exact Hartree result in the form of an integral equation, which may be easier to work with when obtaining exact solution to Eq. (5.7) and (5.8). We utilize the expression for $\Delta V_H(\mathbf{r},\mathbf{r}')$ to calculate a leading order correction to the solution of Eq. (5.9). Provided that the size of the correction remains small, the solution to Eq. (5.9) captures all the important qualitative physics (explained below).

We obtain a partial solution to (5.9) (see Appendix C) of the following form

$$V_H(\mathbf{r},\mathbf{r}) - V_H(\infty,\infty) = \tilde{V}_{Hg}(\mathbf{r},\mathbf{r}) + \delta V_I(\mathbf{r},\mathbf{r}), \tag{5.10}$$

$$\text{where } \delta V_I(\mathbf{r},\mathbf{r}) = \frac{\tilde{\kappa} - \hat{\kappa}(\mathbf{r},0)}{2\pi}, \tag{5.11}$$

$$\tilde{V}_{Hg}(\mathbf{r},\mathbf{r}) = -\frac{2}{(2\pi)^2}\sum_n \int_{-\infty}^{\infty} dq K_n(\hat{\kappa}(\mathbf{r},q)R) K_n(\hat{\kappa}(\mathbf{r},q)R)$$
$$\left[\hat{\kappa}(\mathbf{r},q) I_n'(\hat{\kappa}(\mathbf{r},q)b)\left(I_n(qb) - \frac{K_n'(qa)}{I_n'(qa)} K_n(qb)\right) - q I_n(\hat{\kappa}(\mathbf{r},q)b)\left(I_n'(qb) - \frac{K_n'(qa)}{I_n'(qa)} K_n'(qb)\right)\right]$$
$$\left[\hat{\kappa}(\mathbf{r},q) K_n'(\hat{\kappa}(\mathbf{r},q)b)\left(I_n(qb) - \frac{K_n'(qa)}{I_n'(qa)} K_n(qb)\right) - q K_n(\hat{\kappa}(\mathbf{r},q)b)\left(I_n'(qb) - \frac{K_n'(qa)}{I_n'(qa)} K_n'(qb)\right)\right]^{-1} \tag{5.12}$$

and

$$\hat{\kappa}(\mathbf{r},q) = \sqrt{\tilde{\kappa}^2 \lambda(\mathbf{r}) \cos\phi_0(\mathbf{r}) + q^2}\,. \tag{5.13}$$

In deriving the above expressions we have assumed that $\varepsilon_w \gg \varepsilon_c$, more general expressions may be found in Appendix C. Eq. (5.11) represents a change in hydration energy of an ion moving from a bulk (rescaled) concentration $\tilde{\kappa}^2$ to a (rescaled) local concentration $\hat{\kappa}(\mathbf{r},0)^2$. If $\hat{\kappa}(\mathbf{r},0) > \tilde{\kappa}$, this term is negative. Then, when an ion moves towards the Macro-ion, its overall potential energy is reduced due to neighboring ions being correlated with it. These ions adjust themselves in the field of the ion, essentially creating a correlation hole [48], see Fig. 2. This effect becomes more pronounced when the local density increases as more ions can adjust themselves to that single ion.

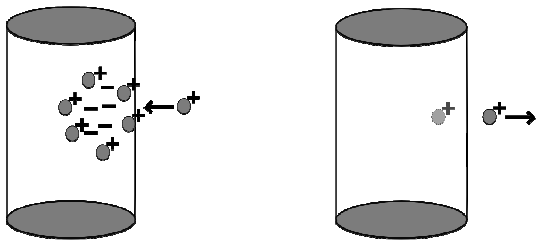

Fig. 2: schematic drawings of correlation effects (left) and image charge effects (right). In the former ions adjust to the field of an ion creating a correlation hole which draws the ion closer to macro-ion. In latter an ion sees its image charge reflection at the dielectric boundary, from which it is repelled.

Eq. (5.11) represents the change in self energy due to image charge effects and exclusion of ions from the core. As an ion moves towards the macro-ion it experiences repulsion due to its image charge. The other ions will try and weaken this effect by adjusting themselves. As the local concentration of ions increases the image charge repulsion is screened out more as more ions can adjust. Also, in Eq. (5.11) there is an exclusion effect. As no ions may penetrate the core, the core region cannot participate in screening out the electrostatic self energy of an ion. So, this exclusion effect is also a positive contribution. This behaves differently from the image charge effect as it increases with local ionic concentration. This is because as the local Debye atmosphere around ion becomes more pronounced, such exclusion of ions has a more profound effect on the self energy.

Through the initial definition of $\lambda(\mathbf{r})$ (Eq. (5.5)) one is able to construct an equation to solve $\lambda(\mathbf{r})$. Then one is left with solving this system of equations numerically for both $\lambda(\mathbf{r})$ and $\phi_0(\mathbf{r})$.

6. Dealing with finite ionic charge distributions

6.1 General formulation

In this section we deal with the more realistic situation of extended charge distributions. We will suppose for simplicity, in the main text, that both species of ions have the same charge distribution $f_+(\mathbf{r}-\mathbf{r}_j^+,\boldsymbol{\omega}_j^+)=f_-(\mathbf{r}-\mathbf{r}_j^+,\boldsymbol{\omega}_j^+)=f(\mathbf{r}-\mathbf{r}_j^+,\boldsymbol{\omega}_j^+)$. Though in reality, their sizes and shapes of both electrolyte species can be quite different.

Using Eqs. (2.1) and (2.13), it is possible to derive a field theory, albeit a non-local one, that takes account of these finite charge distributions.

$$Z_\lambda=\frac{1}{Z_{VAC}}\int \mathfrak{D}\phi(\mathbf{r})\exp\left(-H_{ext}[\phi(\mathbf{r})]/\Xi\right) \tag{6.1}$$

where

$$\begin{aligned} H_{ion}[\phi(\mathbf{r})]=&\int d^3r\left[\frac{1}{4}\chi(\mathbf{r})\left(\nabla\phi(\mathbf{r})\right)^2+i\tilde{\sigma}(\mathbf{r})\phi(\mathbf{r})\right]\\ &-\frac{\tilde{\kappa}^2}{4\Lambda}\int d^3r\int\frac{d^3\omega}{8\pi^2}\Omega(\mathbf{r},\boldsymbol{\omega})\left[2\cos\Phi(\mathbf{r},\boldsymbol{\omega})-e^{-i\Phi(\mathbf{r},\boldsymbol{\omega})}\left(e^{-\tilde{V}_{ch}(\mathbf{r},\boldsymbol{\omega})}-1\right)\right]\end{aligned} \tag{6.2}$$

and

$$\Phi(\mathbf{r},\boldsymbol{\omega}) = \int d^3r' f(\mathbf{r}-\mathbf{r}',\boldsymbol{\omega})\phi(\mathbf{r}'), \qquad \tilde{V}_{ch}(\mathbf{r},\boldsymbol{\omega}) = \int d^3r f_+(\mathbf{r}-\mathbf{r}',\boldsymbol{\omega})V_{ch}(\mathbf{r}') \tag{6.3}$$

Furthermore, we have derived a more generalized field theory that does not assume that both species have the same shape. This can be found in Appendix D.

6.2 Hartree Equations

From such a field theory it is possible to derive differo-integral Hartree Equations (see Appendix D) (for $\tilde{V}_{ch}(\mathbf{r},\boldsymbol{\omega}) = 0$).

$$\chi(\mathbf{r})\nabla_{\mathbf{r}}^2 V_H(\mathbf{r},\mathbf{r}') + \int \frac{d^3\tilde{\omega}}{8\pi^2}\int d^3\tilde{r}\int d^3\tilde{r}'$$
$$\times f(\mathbf{r}-\tilde{\mathbf{r}},\tilde{\boldsymbol{\omega}})\Omega(\tilde{\mathbf{r}},\tilde{\boldsymbol{\omega}})\tilde{\kappa}^2\lambda_{ext}(\tilde{\mathbf{r}},\tilde{\boldsymbol{\omega}})\cosh\Phi_0(\tilde{\mathbf{r}},\tilde{\boldsymbol{\omega}})\, f(\tilde{\mathbf{r}}-\tilde{\mathbf{r}}',\tilde{\boldsymbol{\omega}})V_H(\tilde{\mathbf{r}}',\mathbf{r}) = -2\delta(\mathbf{r}'-\mathbf{r}) \tag{6.4}$$

$$\chi(\mathbf{r})\nabla^2\phi_0(\mathbf{r}) - \int d^3r'\int \frac{d^3\omega'}{8\pi^2} f(\mathbf{r}-\mathbf{r}',\boldsymbol{\omega}')\Omega(\mathbf{r}',\boldsymbol{\omega}')\tilde{\kappa}^2\lambda_{ext}(\mathbf{r}',\boldsymbol{\omega}')\sinh\Phi_0(\mathbf{r}',\boldsymbol{\omega}') = -2\tilde{\sigma}(\mathbf{r}), \tag{6.5}$$

where $\Phi_0(\mathbf{r},\boldsymbol{\omega}) = \int d^3r' f(\mathbf{r}-\mathbf{r}',\boldsymbol{\omega})\phi_0(\mathbf{r}')$, the potential energy of an ion, with orientation $\boldsymbol{\omega}$, in the average field produced by the macro-ion and the other small ions. Here again, there is a Boltzmann weight associated by the change in self energy of an ion as it moves towards the macro-ion. This is

$$\lambda_{ext}(\mathbf{r},\boldsymbol{\omega}) = \exp(-\Xi\left(E_H(\mathbf{r},\mathbf{r},\boldsymbol{\omega}) - E_H(\infty,\infty,\boldsymbol{\omega})\right)/2), \tag{6.6}$$

where $E_H(\mathbf{r},\mathbf{r},\boldsymbol{\omega}) = \int d^3r''\int d^3r''' f(\mathbf{r}-\mathbf{r}'',\boldsymbol{\omega})V_H(\mathbf{r}'',\mathbf{r}''')\, f(\mathbf{r}''-\mathbf{r}',\boldsymbol{\omega})$ is the ionic self energy for an ion with orientation $\boldsymbol{\omega}$. In the Hartree approximation the local concentration of ions (with a given orientation $\boldsymbol{\omega}$), and the ionic charge density are given by $c(\mathbf{r},\boldsymbol{\omega}) = \lambda(\mathbf{r},\boldsymbol{\omega})\cosh\Phi_0(\mathbf{r},\boldsymbol{\omega})$ and $\rho(\mathbf{r}) = \int d^3\omega\int d^3r' f(\mathbf{r}-\mathbf{r}',\boldsymbol{\omega})\lambda(\mathbf{r}',\boldsymbol{\omega})\sinh\Phi_0(\mathbf{r}',\boldsymbol{\omega})$, respectively.

By way of solving and approximating these Hartree equations we shall consider only the simplest case of a spherically symmetric charge distribution, i.e. one that does not depend on $\boldsymbol{\omega}$ [49]. Then $\boldsymbol{\omega}$ may be simply integrated out and here on we will drop $\boldsymbol{\omega}$ from our results. Then, these equations considerably simplify. Now, by choosing an appropriate form for $f(\mathbf{r}'-\mathbf{r})$ considerable analytic progress can be made in solving them. We choose

$$f(\mathbf{r}'-\mathbf{r}) = \frac{1}{4\pi}\frac{1}{r_{ion}^2}\frac{1}{|\mathbf{r}-\mathbf{r}'|}\exp\left(-|\mathbf{r}-\mathbf{r}'|/r_{ion}\right). \tag{6.7}$$

Indeed, such a distribution does not accurately describe the charge distribution of a small ion, but Eq. (6.7) may still describe the physics. The term $E_H(\mathbf{r},\mathbf{r})$ may be divided into two pieces $E_{Hg}(\mathbf{r},\mathbf{r})$ (analogous to $\tilde{V}_{Hg}(\mathbf{r},\mathbf{r})$) that describes image charge effects and $\delta E_I(\mathbf{r},\mathbf{r})$ (analogous to $\delta\tilde{V}_I(\mathbf{r},\mathbf{r})$) that describes local changes in the electrostatic self energy of an ion due to the varying concentration. Now, any charge smearing causes a reduction in $\tilde{E}_{Hg}(\mathbf{r},\mathbf{r})$, which is captured in Eq. (6.7). Also, for the small values of r_{ion}, which we consider $\Phi_0(\tilde{\mathbf{r}}) \approx \phi_0(\tilde{\mathbf{r}})$, here the charges may be considered point like and the actual form of the charge distribution does not matter. Lastly, the term most sensitive to finite size effects is $\delta E_I(\mathbf{r},\mathbf{r})$. Here they do make quite a difference. This term is essentially is a localized solvation energy. Then it might be better consider finite size effects in this term using some modification of the Born approximation, to take account of the fact that other ions and solvent molecules cannot penetrate into the ion. Therefore, possibly a better choice of $f(\mathbf{r}'-\mathbf{r})$ might be to consider an effective charge distribution of a uniformly charged shell (or a smeared charged shell) with the same radius of that of the ion [17]. However, the resulting equations are much harder to work with, and so we have not considered this. Indeed Eq. (6.7) may work reasonably, provided that the parameter r_{ion} is correctly related to ionic size. Indeed, the big advantage of (6.7) is that it is possible to derive an approximate partial solution to Eq. (6.4) as shown in Appendix D, by making the same WKB like approximation. The result is, however, rather cumbersome so we refrain from quoting it the main text. But this again leaves us with a very much simplified integral equation on $\lambda_{ext}(\mathbf{r})$ which can be easily solved numerically in conjunction with the mean field.

7. Results for the uniformly charged macro-ion with no chemi-adsorption.

7.1 Point Charges

In these calculations, we consider only mono-valent ions and calculate both the correlation parameter and Gouy-Chapman lengths for a surface charge density of $\sigma = 16.8\mu\text{C/cm}^2$, that for DNA. For which we find values of $\Xi \approx 20$ [50] and $\mu \approx 2.2\text{Å}$. For different charge densities, comparable with DNA, it is more convenient to keep these values fixed, instead of recalculating them for each charge density.

In what follows, we will suppose a uniform charge distribution on the macro ion so that $\tilde{\sigma}(\mathbf{r}) = \tilde{\sigma}(R) = -\sigma_f \delta(R-a)$, here we take $0 \le \sigma_f \le 1$. The quantity σ_f represents a fraction of the DNA charge density. So, we may consider different σ_f and keep Ξ and μ fixed. We take the radius of the core region to be $a = 4.54$ Gouy-Chapman lengths ($\approx 10\text{Å}$), roughly that of a DNA molecule. We allow the closest approach distance from the central axes of the macro-ion, for the small ions, to be $b = 5.91$ (in μ). Therefore, we assign each ion an effective hard core radius of 1.37μ ($\approx 3\text{Å}$). This roughly corresponds to a small ion (for instance sodium) surrounded by a tightly bound first

hydration shell of water. The key assumption being: the electrostatic field is not strong enough to partially remove this hydration shell from a significant fraction of ions close to the macro-ion.

Before working with the equations numerically, it is convenient to recast them in an integral equation form. We may define a quantity called the excess charge density, $\rho_{ex}(R)$ so that

$$\chi(R)\left[\frac{d^2\phi_0(R)}{dr^2}+\frac{1}{r}\frac{d\phi_0(R)}{dr}\right]-\Omega_I(R)\tilde{\kappa}^2\phi_0(R)=-2\tilde{\sigma}(R)+\rho_{ex}(R) \tag{7.1}$$

It is then possible to show that $\rho_{ex}(R)$ must satisfy the following integral equation

$$\begin{aligned}\rho_{ex}(R)&=\kappa^2\int dR'\bar{G}(R,R')\left(\frac{2\sigma_f a}{b}\delta(R'-b)+\rho_{ex}(R')\right)\\&-\kappa^2\lambda(R)\sinh\int dr'\bar{G}(R,R')\left(\frac{2\sigma_f a}{b}\delta(R'-b)+\rho_{ex}(R')\right),\end{aligned} \tag{7.2}$$

where

$$\bar{G}(R,R')=\hat{G}(R,R')\theta(R-R')+\hat{G}(R',R)\theta(R'-R)\,, \tag{7.3}$$

and

$$\hat{G}(r,r')=\frac{2r'K_0(\tilde{\kappa}r)}{K_1(\tilde{\kappa}a)}\left(K_0(\tilde{\kappa}r')I_1(\tilde{\kappa}a)+I_0(\tilde{\kappa}r')K_1(\tilde{\kappa}a)\right). \tag{7.4}$$

The mean electrostatic potential is determined through

$$\phi_0(R)=\int_{-\infty}^{\infty}dr\bar{G}(R,R')\left(2\sigma(R')+\rho_{ex}(R')\right). \tag{7.5}$$

Using our approximation, our equation on $\lambda(R)$ reads as

$$\lambda(R)=\exp(-\Xi/2(\tilde{V}_{Hg}(R,R)+\delta V_I(R,R)))\,, \tag{7.6}$$

where $\delta V_I(R,R)$ and $\tilde{V}_{Hg}(R,R)$ are given by Eqs (5.11) and (5.12), respectively. Now $\hat{\kappa}(\mathbf{r},q)$ depends spatially only on R through $\lambda(R)$ and $\phi_0(R)$. As well as solving both numerically these two equations (((7.2)) and((7.6))), we solve Eq. (7.2) with $\lambda(R)=1$; this corresponds to the P-B equation.

In numerically solving these equations we use an iterative technique. We start with initial guesses (trial functions) for both $\lambda(R)$ and $\rho_{ex}(R)$, $\lambda_0(R)$ and $\rho_0(R)$. These are then fed into the RHS of both Eq. (7.2) and (7.6), and new values $\lambda_1(R)$ and $\rho_1(R)$ are obtained from the LHS of both equations. Due to the strong non-linear nature of these equation we then use a particular algorithm to improve the convergence rate [51]. Instead of $\rho_1(R)$ we use $\bar{\rho}_1(R) = 0.5\rho_1(R) + 0.5\rho_0(R)$. Both $\lambda_1(R)$ and $\bar{\rho}_1(R)$ are then inserted back into the RHS of Eqs. (7.2) and (7.6), so $\lambda_2(R)$ and $\bar{\rho}_2(R)$ are calculated. One then iterates the process. But, crucially at the n-th step, one uses the values $\lambda_{n-1}(R)$ and $\bar{\rho}_{n-1}(R) = 0.5\bar{\rho}_{n-2}(R) + 0.5\rho_{n-1}(R)$ to calculate both $\lambda_n(R)$ and $\rho_n(R)$. We iterate as many times as is required to obtain accurate values of $\lambda(R)$ and $\rho_C(R)$. This achieved when $\lambda_n(R) \simeq \lambda_{n-1}(R)$ and $\rho_n(R) \simeq \rho_{n-1}(R)$, which we insure to a high accuracy.

7.2 Extended Charges

Again we consider uniform charge distribution on the macro ion, again of the same form. One can introduce radial smearing of the fixed charge groups. But for simplicity, and purposes of comparison, we keep the same charge distribution as before.

The ionic potential energy $\Phi_0(R)$ is determined through

$$\Phi_0(R) = \int_0^\infty R' dR' \bar{\mathcal{G}}(R, R') \eta(R') \tag{7.7}$$

an explicit expression for the Green's function $\bar{\mathcal{G}}(R, R')$ is cumbersome and is left to Appendix D. The quantity $\eta(R')$ may be determined self-consistently through

$$\eta(R) = \kappa^2 \int_0^\infty dR' R' \bar{\mathcal{G}}(R, R') \eta(R') - \kappa^2 \lambda(R) \sinh \int_0^\infty dr' r' \bar{\mathcal{G}}(R, R') \eta(R'), \qquad \text{for } R > b \tag{7.8}$$

$$\eta(R) = \left[-\frac{d^2}{dR^2} - \frac{1}{R}\frac{d}{dR} + \frac{1}{r_{ion}^2} \right] 2\tilde{\sigma}(R) \qquad \text{for } R < b. \tag{7.9}$$

Now, $\lambda(R)$ ($\lambda_{ext}(R)$ in previous section) is self consistently determined through

$$\lambda(R) = \exp(-\Xi / 2(\tilde{E}_{Hg}(R, R) + \delta\tilde{E}_I(R, R))), \tag{7.10}$$

where expressions for $\tilde{E}_{Hg}(R, R)$ and $\delta E_I(R, R)$ (in terms of $\lambda(R)$) are given in Appendix D.

In the limit $r_{ion} \to 0$, Eqs. (7.7) ,(7.8) and (7.10) reproduce Eqs. (7.5), (7.2) and (7.6). These equations are solved in an iterative manner similar to those of the point charges.

The difference is that instead of using $\rho_{ex}(R)$, $\eta(R)$ is used as well as $\lambda(R)$ in the iterative procedure.

For the size of our charge distributions, we consider $r_{ion} = 0.185$ and $r_{ion} = 0.25$ (sizes given in Gouy-Chapman lengths) [52]. Not very large values of r_{ion} are chosen for the following reason. As the charge distribution of the small ions becomes very smeared out, some quite non-trivial behaviour is expected. There is a possibility for such sizes, that there will be oscillatory behavior in the solutions of Eqs. (7.8) and (7.10) . This is because, at sufficiently large values of r_{ion}, two of the three decay lengths present in both $\bar{\mathcal{G}}(r,r')$ and $E(\mathbf{r}',\mathbf{r})$ may become complex (see Appendix D). This change in the decay lengths has not been taken account of in numerical calculations [53].

7.3 Results for electrostatic potential

We obtain solutions both for different values of σ_f and $\tilde{\kappa}$. In Fig.3 we present results for ionic potential energy $\Phi(R)$ (the potential energy of an small ion in the mean field $\phi_0(R)$) calculated with $r_{ion} = 0.185$ and $\tilde{\kappa} = 0.48$ for various values of σ_f. As expected, we see that $\Phi(R)$ increases with increasing σ_f and falls away to zero as $R \to \infty$.

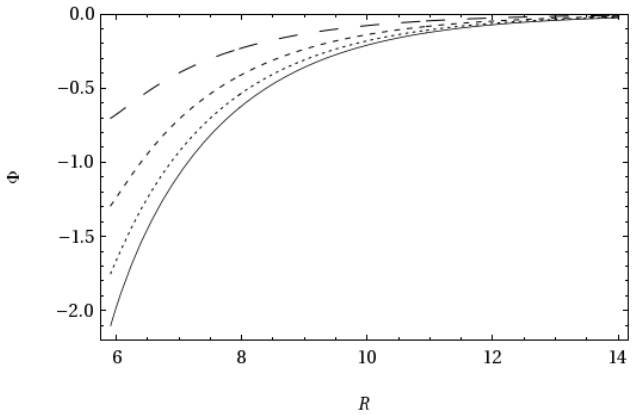

Fig.3: Figure showing the ionic potential energy, Φ as a function of distance away from the central axes of the macro-ion, for $\tilde{\kappa} = 0.48$, $r_{ion} = 0.185$; with 100% (solid Line), 75% (dotted line), 50% (short dashes) and 25% (long dashes) of DNA charge.

In Fig.4 we calculate the mean electrostatic potential using the PB equation, as well as the Modified PB equations for point charges and finite r_{ion}. One immediate observation is that, close to the macro-ion, the field differs slightly between these four types of solution. The size relative differences between these four types of solution are mainly dependent on σ_f and depend not so much on $\tilde{\kappa}$ in the range of values explored ($0.32 \le \tilde{\kappa} \le 0.48$). The difference increases slightly with increasing σ_f. Only for the value $\sigma_f = 1$, do we see a appreciable difference. The magnitude of the potential is smallest for point charges calculated using the modified PB equation. Here, the largest magnitude is for the PB equation ($\lambda(R) = 1$). The curves for both extended charge

distributions lie within these two, with $r_{ion} = 0.25$ providing a very slightly larger magnitude of the potential than $r_{ion} = 0.185$. Indeed, the finite size makes the solutions more like the PB equation. The main effect of $\tilde{\kappa}$ is to push up ϕ when its value is decreased.

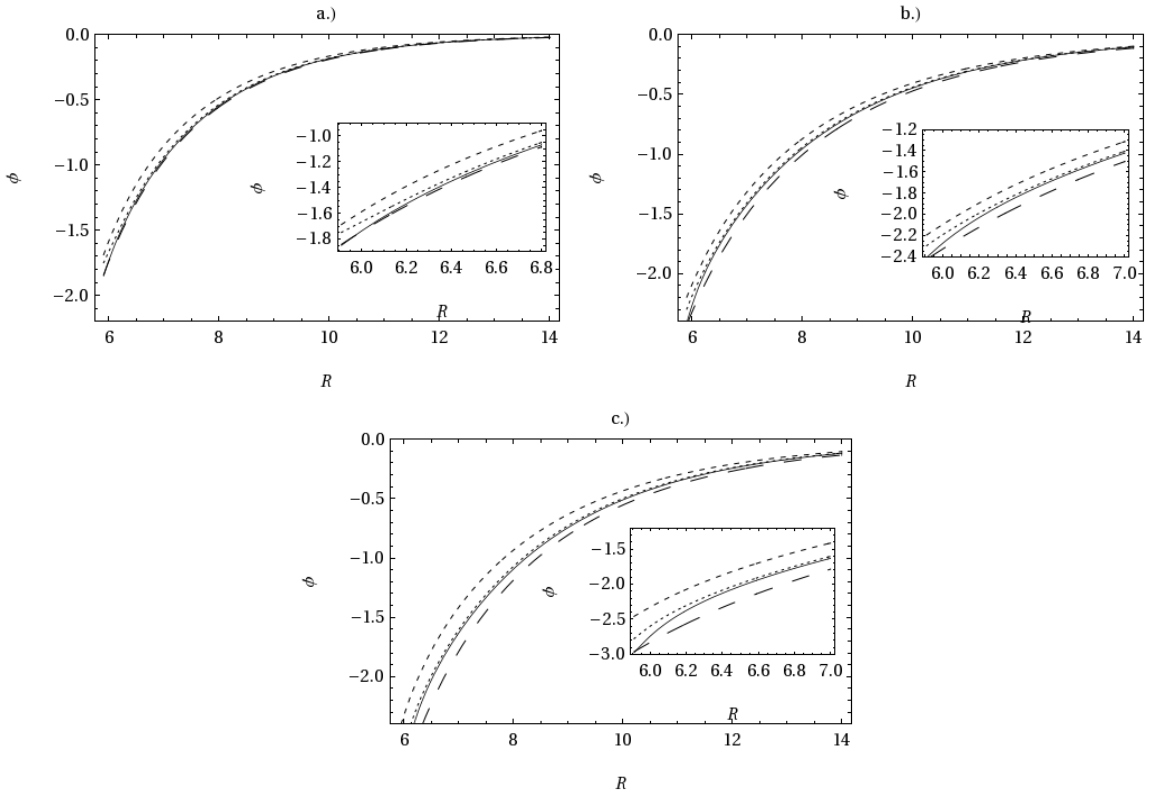

Fig.4: the electrostatic potential for a.) $\tilde{\kappa} = 0.48$ b.) $\tilde{\kappa} = 0.4$ and c.) $\tilde{\kappa} = 0.32$; the first two are calculated at 75% of the DNA charge density, the last with 100% on the Macro-ion; using standard PB equation (long dashes), modified PB equation for point charge ions (short dashes), modified PB equation for $r_{ion} = 0.185$ (dotted line), and for $r_{ion} = 0.25$ (solid line). Each inset shows a magnification of its main graph.

7.4 The correlation parameter $\lambda(R)$

In Fig. 5 we calculate $\lambda(R)$ with $r_{ion} = 0.185$ at the values $\tilde{\kappa} = 0.48$ and $\tilde{\kappa} = 0.32$ for various values of σ_f. When σ_f is small, $\lambda(R)$ simply decreases with decreasing separation. Here, the effect of image charge repulsion (the term $\tilde{V}_{Hg}(R,R)$ for point charges) dominates over correlation effects ($\delta V_I(R,R)$ for point charges). The image charge repulsion makes it less energetically favorable for an ion to be close to the surface of the macro-ion, as it sees an 'image' charge reflection of itself on the macro-ion surface, which effectively is a charge of the same sign. This repulsion essentially assigns a smaller value of the Boltzmann weight $\lambda(R)$ near the surface.

As one starts to increase σ_f, in certain places, $\lambda(R)$ starts to become greater than one in certain places and a peak develops. Ions are able to correlate, or adjust themselves, so as to screen each other's electrostatic self-energy. To put it another way, a positive ion 'sees' correlation holes from the displacement of other positive ions in its vicinity. These 'holes' help to increase the attraction it sees from the surface of the macro-ion (see Fig.2). This effectively pushes up the Boltzmann weight; $\lambda(R)$ becomes larger. As the local density of ions increases the correlation effects become stronger, as more ions can adjust to the field of one ion. Provided that σ_f is sufficiently large, as one moves closer to the molecule the density does increase. This provides positive feedback, as a higher density draws more ions which push up the density. However, thermal effects, image charge effects and the adjustment of the mean electrostatic potential, due to a larger number of ions near the surface, prevent too many of the ions being drawn to the immediate vicinity of the macro-ion. At a certain point image charge effects start to win out over correlation function effects and $\lambda(R)$ does indeed start to become smaller with decreasing R.

One thing to notice that these correlation effects seem to be more pronounced at $\tilde{\kappa} = 0.32$ than at $\tilde{\kappa} = 0.48$. This may seem to run counter to the previous discussion. Certainly, the ionic correlation effects should be greater at $\tilde{\kappa} = 0.48$ for an ion in the bulk. Here, the stronger Debye atmosphere reduces an ion's hydration energy. But one should point out, $\lambda(R)$ is a measure of the change in the ion's electrostatic self-energy going from the bulk to the vicinity of the macro-ion. Therefore, the only correlation effects that are considered are due to the increase in the local charge density near the macro-ion. Because the ratio of ionic local density over bulk density is much larger in $\tilde{\kappa} = 0.32$ is larger than in $\tilde{\kappa} = 0.48$, these correlation effects are more pronounced. In turn, this yields a larger $\lambda(R)$.

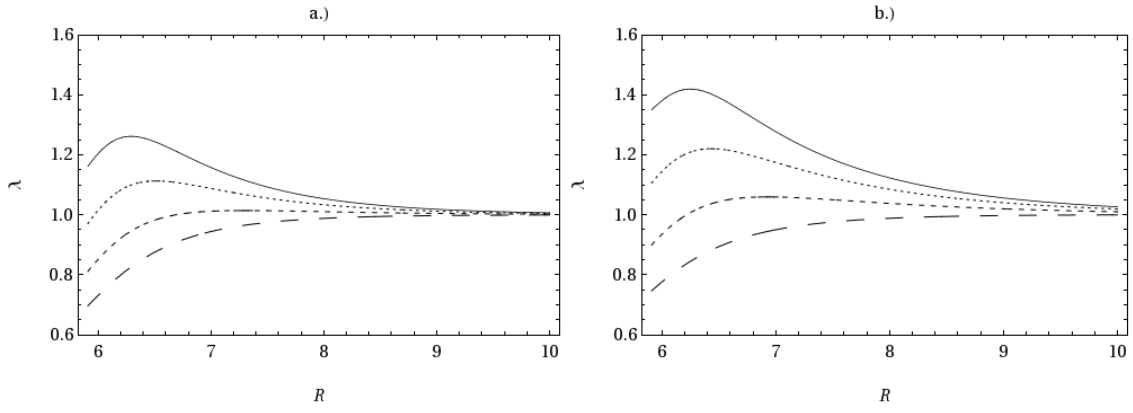

Fig.5: λ calculated for a.) $\tilde{\kappa} = 0.48$ and b.) $\tilde{\kappa} = 0.32$ for various values of macro-ion charge density with $r_{ion} = 0.185$. The chosen values are 100% (solid Line), 75% (dotted line), 50% (short dashes) and 25% (long dashes) of the DNA charge density.

In Fig. 6 we compare $\lambda(R)$ calculated for different sizes of ionic charge distribution for the value $\sigma_f = 0.75$. We see a dramatic reduction in $\lambda(R)$ when we assign the ion a finite size charge distribution. Correlation effects are much reduced. This is because at close distances, in the vicinity of a small ion, the electrostatic forces on other ions are very much reduced. Consequently, they are less able to screen out the self energy of a small ion. However, when $\sigma_f = 0.25$, $\lambda(R)$ is completely dominated by image charge effects and the finite size effects are less profound. Nevertheless, at close distances the degree of image charge repulsion a point ion sees from the surface of the macro-ion is larger than an ion with an extended charge distribution. Therefore, as seen in the results, $\lambda(R)$ is smallest for the point charges, increasing with increasing ionic charge radius. Further out, the point like ions benefit more from correlation effects, which leads to point ions having the largest value of $\lambda(R)$. Where these curves cross depends on salt concentration. At low salt concentrations, presumably, the increased correlation effects, due to a greater relative density of ions to that of the surrounding bulk solution, cause this separation to occur at smaller R.

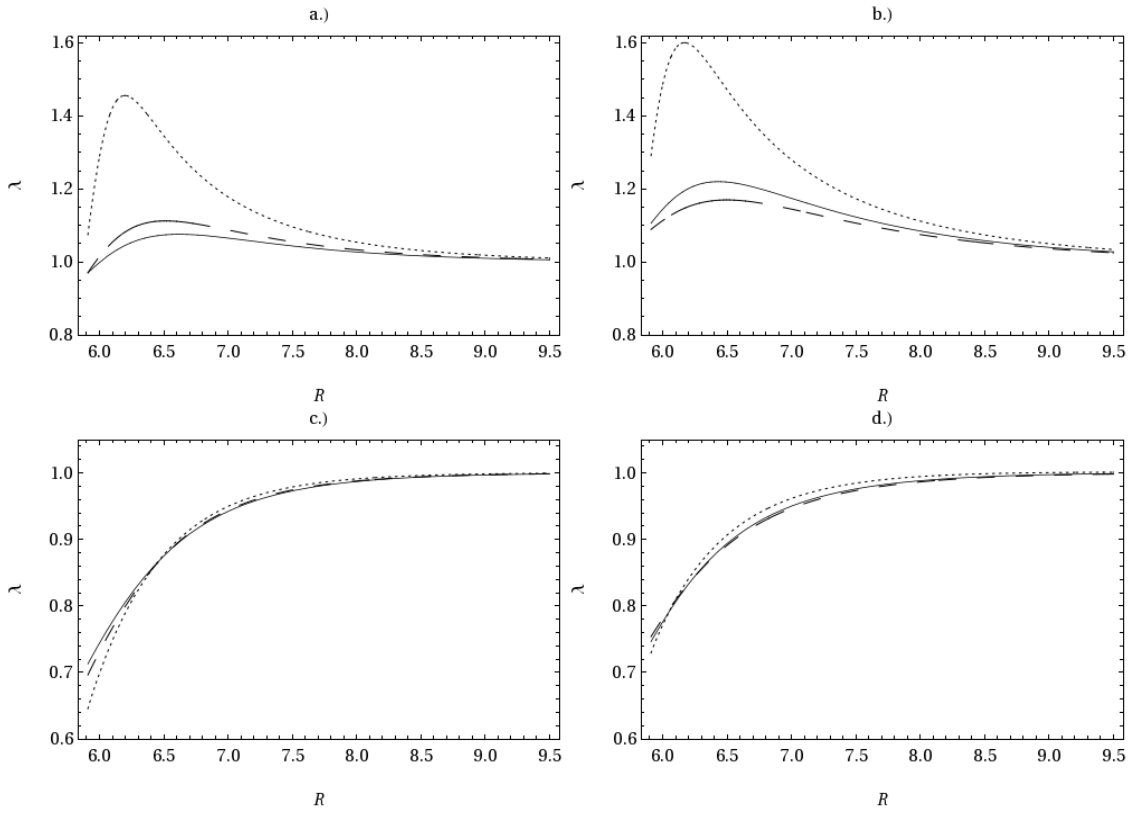

Fig. 6: comparison of λ calculated for point charges (dots), $r_{ion} = 0.185$ (dashes) and $r_{ion} = 0.25$ (solid line). The first two graphs are for 75% of the DNA charge density; a.) calculated at $\tilde{\kappa} = 0.48$ and b.) calculated at $\tilde{\kappa} = 0.32$. The second set of graphs are for 25% of the DNA charge density; c.) calculated, again, at $\tilde{\kappa} = 0.48$ and d.) calculated at $\tilde{\kappa} = 0.32$.

7.5 Results for local concentration of ions and charge density.

In Fig.7 we show calculations of the local concentration of small ions around the macro-ion divided by the bulk concentration, both for the PB equation and modified PB equations. Indeed, as we would expect for the PB equation, for lower bulk salt concentrations this relative quantity is much larger. Between the values of $\sigma_f = 0.75$ (a.) and b.)) and $\sigma_f = 0.25$ (c.) and d.)) we see major qualitative differences.

At $\sigma_f = 0.75$, the general trend for all the concentrations is to increase with decreasing R. All the modified PB curves more or less follow the density curve for the PB equation. Nevertheless, the density distribution of the modified PB equation for point charges shows a peak. Of the four curves, the relative concentration is lowest for the PB equation due to no correlation effects. The concentration calculated with the modified PB equation has the highest concentration, because it has the strongest correlation effects.

But, for $\sigma_f = 0.25$ the situation is much different. There is a large relative discrepancy between the concentration calculated with the PB equation and those with the modified PB equation. At small values of R, the local concentration decreases with decreasing R for the modified PB equation. This discrepancy is entirely due to image charge effects, which dominate at these charge densities.

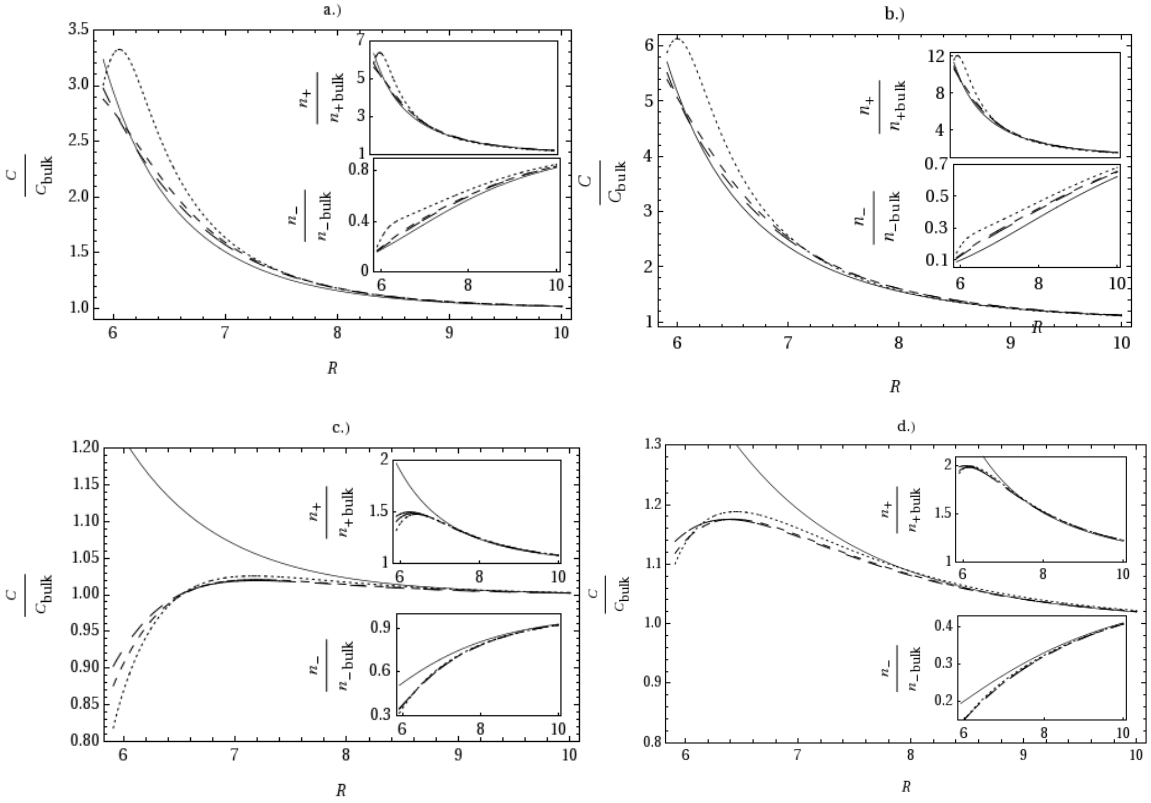

Fig.7: shows calculations of the local number concentration, c divided by the bulk concentration, c_{bulk} of small ions near the macromolecule a function of distance away from the central axes, R. The insets show

the individual number concentrations of positive, n_+ and negative ions, n_-, divided by their bulk concentrations, as functions of R. These densities are calculated using the PB equation (solid line), modified PB equation for point charges (dotted line), modified PB equation for $r_{ion} = 0.185$ (long dashes) and $r_{ion} = 0.25$ (short dashes).

In Fig.8 we show calculations of the charge density of the small ions. The extended distributions penetrate into the region $a < R < b$. This allowed for the finite charge distributions; the only requirement is that the ionic centers lie outside $R = b$. Indeed, the tail, for small R in the charge density, is due individual charge distributions of each ion at $R > b$ decaying away exponentially. Very little of the charge distribution penetrates into the macro-ion core, therefore an assumption (Appendix D) which is used in solving the modified PB equation for ions with extended charge distributions is completely justified. In the insets we also show the excess charge distribution ρ_{ex}. This excess charge is neglected when equations are fully linearized and $\lambda(R) = 1$. We see that at $\sigma_f = 0.25$, neglecting ρ_{ex} may be an adequate approximation, but for $\sigma_f = 0.75$ this approximation does not work well in all cases.

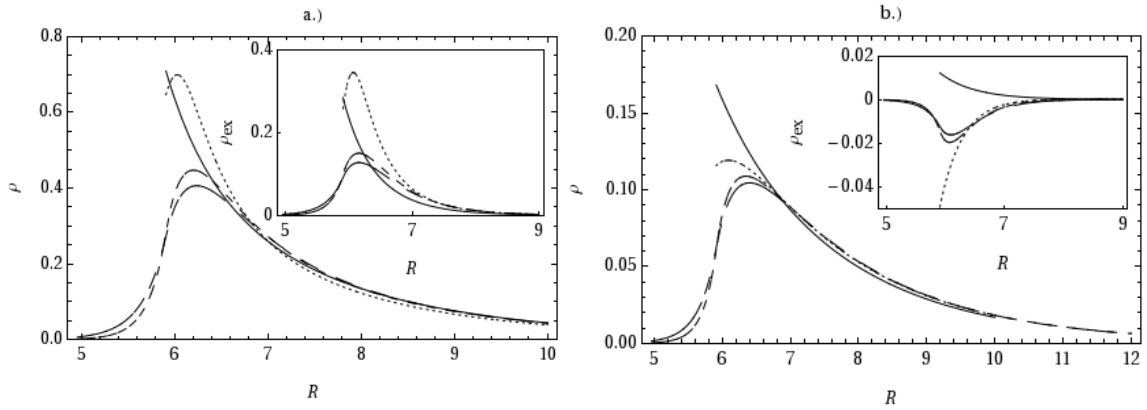

Fig.8: shows the calculated full charge densities (main graph) and excess charge densities (inset) for $\tilde{\kappa} = 0.48$; calculated at a.) 75% and b.) 25% of the DNA charge density; using PB equation (solid line), modified PB equation for point charges (dotted line), $r_{ion} = 0.185$ (medium dashes) and $r_{ion} = 0.25$ (long dashes).

7.6 Effective interaction between two uniformly charged cylinders

We may write down the following effective pair potential [1], here written in normal SI units of length

$$\frac{V_{\text{int}}}{Lk_BT} = 2(1-\theta)^2 \frac{l_B}{l_c^2}\left(\frac{K_0(\kappa_D R) + \Omega(\kappa_D R, \kappa_D a)}{(\kappa_D a)^2 \left[K_1(\kappa_D a)\right]^2} \right) \tag{7.11}$$

where

$$\Omega(x,y) = -\sum_{j=-\infty}^{\infty} K_j(x)^2 \frac{I_j'(y)}{K_j'(y)}. \tag{7.12}$$

Here l_c is the distance between two fixed charge groups on the macro ion divided by their charge and is related to the surface charge density $l_c = (2\pi\sigma_s a)^{-1}$. The first term in Eq. (7.11) represents the direct electrostatic interaction between the Macro-ions, which is enhanced by the low dielectric cores by a factor of $(\kappa_D a)^{-2}\left[K_1(\kappa_D a) I_0(\kappa_D a)\right]^{-2}$. The second term represents an image charge repulsion term, where both the excess counter-ions and fixed charges are repelled by their image charges on the surface of the other macro-ion. As yet, this expression does not contain any attractive term for correlation effects, as well as accounting for adjustment of ions in the charge compensation; these certainly will have some effect as the cylinders are brought closer together. Though, for univalent ions former term may be small compared to the other terms in the interaction. But, this still remains to be shown.

On examination of the excess charge densities in Fig.8, we see that, at an inter-axial separation of $R \gtrsim 14$ (30 Å), the repulsive part of the interaction between two uniformly cylindrical ions with charge density $\sigma_f = 0.75$ in a salt solution with $\tilde{\kappa} = 0.48$ (a Debye screening length $\lambda \simeq 4.58$Å) may be adequately described through Eq (7.11). And, for all other values of the parameters, this approximation (for the repulsive interaction) should work when the excess charge distributions of the two Macro-ions do not overlap, or are negligible so that $\theta \approx 1$.

For the single macro-ion we are able to calculate θ. The parameter θ is related to ρ_{ex} through the following expression (in rescaled units)

$$\theta = \frac{\tilde{k}}{2\sigma_f} \int_0^{\infty} r dr \left[I_0(\tilde{\kappa} r) K_1(\tilde{\kappa} a) + I_1(\tilde{\kappa} a) K_0(\tilde{\kappa} r) \right] \rho_{ex}(r). \tag{7.13}$$

Eq. (7.13) allows us to compute the effective interaction of two uniformly charged marco-ions with low dielectric cores at large distances. In Tables 1 and 2 we show calculated values for the charge compensation parameter for $\tilde{\kappa} = 0.32$ and $\tilde{\kappa} = 0.48$, respectively .

σ_p value	PB equation	Point Charges	$r_{ion} = 0.185$	$r_{ion} = 0.25$
0.25	$\theta = 0.044$	0.0043	-0.0014	-0.0023
0.5	0.146	0.194	0.161	0.157
0.75	0.259	0.379	0.314	0.301
1	0.362	0.528	0.434	0.417

Table 1: Calculated values of θ at $\tilde{\kappa} = 0.32$ ($\kappa_D \approx 0.14 \text{Å}^{-1}$) calculated for the various sizes of ions used in the modified PB equations as well as the PB equation.

σ_p value	PB equation	Point Charges	$r_{ion} = 0.185$	$r_{ion} = 0.25$
0.25	$\theta = 0.030$	-0.066	-0.0014	-0.0023
0.5	0.108	0.140	0.161	0.157
0.75	0.207	0.357	0.314	0.241
1	0.306	N.S	0.434	0.370

Table 2: Calculated values of θ at $\tilde{\kappa} = 0.48$ ($\kappa_D \approx 0.22 \text{Å}^{-1}$) calculated for the various sizes of ions used in the modified PB equations as well as the PB equation. Here N.S means that no solution was obtained.

In the tables we see trends that correspond to trends seen in the graphs of Fig. 4. We see more of an appreciable difference in θ than in the graphs, simply because of their scale; only at large distances do differences in ϕ become significant. For $\sigma_p = 0.25$ we see that the modified PB equations give charge compensations lower than that calculated with the PB equation. This is because of the effects of image charge repulsion. Indeed, θ can be slightly negative, resulting in a slight enhancement of the fixed surface charge density. As is expected, as one increases σ_p the charge compensation increases. Decreasing the screening length also increases the compensation. For $\sigma_p = 0.5$ and the larger values of σ_p, the modified PB equation for point ions gives the largest value of the compensation. This enhancement in the compensation is due to the correlation effects [48]. These compensation values decrease as the more spread out the distribution of charge on the small ions becomes.

7.7 First order corrections

We may compute first correction to the WKB like approximation employed in numerical calculations of this paper and the exact Hartree approximation. Here, we have done so only for point ion distributions. As for extended charge distributions, though completely feasible is a little more involved, and so has not been done. The correction is given by

$$\Delta\tilde{V}_H(\mathbf{r},\mathbf{r}) = -\frac{\tilde{\kappa}^2}{2}\int d^3r''\tilde{V}_H(\mathbf{r},\mathbf{r}'')\Omega_I(\mathbf{r}'')\left(\lambda(R'')\cosh\phi_0(R'') - \lambda(R)\cosh\phi_0(R)\right)\tilde{V}_H(\mathbf{r}'',\mathbf{r}) \quad (7.14)$$

In Appendix C we recast Eq. (7.14) in a more explicit, but cumbersome way, which can readily be used for numerical calculation.

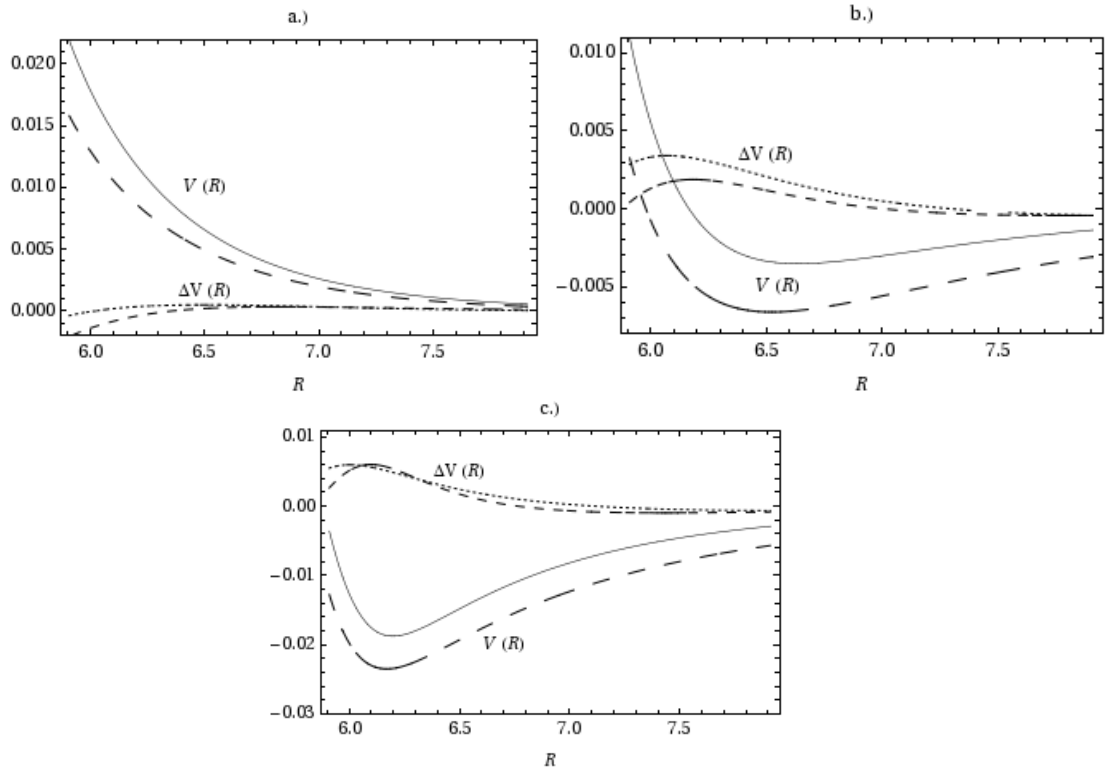

Fig.9 Figures showing both the correction $\Delta V(R) = \Delta\tilde{V}_H(R,R)/2$ and $V(R) = (\tilde{V}_H(R,R) - \tilde{V}_H(\infty,\infty))/2$ for a.) $\sigma_p = 0.25$, b.) $\sigma_p = 0.5$ and c.) $\sigma_p = 0.75$. The quantity $V(R)$ is plotted with solid line (for $\tilde{\kappa} = 0.48$) and the long dashed line (for $\tilde{\kappa} = 0.32$). Whereas the correction is plotted using a short dashed line (for $\tilde{\kappa} = 0.48$) and dotted line (for $\tilde{\kappa} = 0.32$).

In Fig. 9 we show the correction $\Delta\tilde{V}_H(\mathbf{r},\mathbf{r})$ in comparison to $\tilde{V}_H(\mathbf{r},\mathbf{r}) - \tilde{V}_H(\infty,\infty)$. As one sees the correction, for the values considered it is generally quite small in relation to $\tilde{V}_H(\mathbf{r},\mathbf{r}) - \tilde{V}_H(\infty,\infty)$. Though, as we increase the surface charge density we expect its relative size to increase. Also, we see that WKB like approximation works less well in situations where both image charge effects and correlation effects are of similar size, as in the case of $\sigma_p = 0.5$. Here, there are small regions in R where the correction is of similar size or larger due to the fact that $\tilde{V}_H(\mathbf{r},\mathbf{r}) - \tilde{V}_H(\infty,\infty)$ changes sign as the two effects compete. Nevertheless, the overall conclusion, here, is that the WKB like approximation does not perform badly, and certainly is sufficient give insight into the qualitative physics. Of course, better quantitative accuracy can be sought by either incorporating the correction $\Delta\tilde{V}_H(\mathbf{r},\mathbf{r})$ into the calculation of the electrostatic potential or

working with the exact Hartree equations, in an integral equation form, from which the WKB like approximation could form a suitable starting point (see Appendix C for point charges).

8. Discussion

In the numerical solution of the simplified equations, so far, only univalent ions have only been considered. It is possible to consider divalent ions, where the effects are likely to become much more pronounced. But, care here should be taken with the WKB like approximation. It may only work well, here, for relatively small surface charge densities, compared to DNA. Also, as the valance of ions is increased, we expect the Hartree equations, themselves, to work less well. Certainly, for trivalent point like ions, we expect the Hartree approximation to breakdown, close to the surface of the macro-ion. Near the surface, a strong coupling regime [3] will hold, as Ξ is so high. Yet, the situation may be a little more subtle for real ions with valences larger than, or equal to, three. These really cannot be considered to be point like [1,54]. And as we have seen, for extended distributions the correlation and image charge effects can reduce quite markedly.

For the interaction of two cylinders we have calculated the charge compensation parameter θ. Indeed, image charge effects push down this parameter and correlation effects push it up. In the case of a molecule like DNA the inter-axial separation above which this approximation is valid (for $\sigma_p = 1$) may be too conservative for two reasons. The first is that DNA is not a smooth cylinder; it has grooves in which ions may sit accommodating their hydration shells. The second is that chemi-adsorption is important for many species of ion, even mono-valent alkali metals (for example Na^+) feel the presence of fractional charges on the base pairs within the grooves [1]. Chemi-adsorption will bring more ions closer to the macro-ion surface, and this in turn should reduce the separation above which this effective (repulsive) interaction is valid. But, of course the full effective interaction has yet to include an attractive term due to correlation effects.

Indeed, the role of chemi-adsorption is still missing in the numerical calculations. This can be included in the simple case of a very short ranged potential. Here, we may assume an excess bound fraction of counter-ions at $r = b$, $\rho_b(b)$. This supposes that the chemi-adsorption happens through the hydration shell and that there is no chemi-adsorption directly with the ions. The former has to be strong enough to partially remove the hydration shells of a considerable fraction of the ions [55]. Then excess charge density, due to this bound fraction, takes the form $\rho_b(b) = \left(\exp(-V_c / k_B T) - 1\right)\exp(-\phi)$ (for point charges). However, solving for $\rho_b(b)$ is more complicated than simply adsorbing this term into σ_p and then varying σ_p, in the calculations, to arrive at the correct ϕ for a particular value of V_c. This is because these bound charges *are not fixed.* In principle, they should *adjust* to ions outside this layer, again creating correlation effects. Therefore, the excess charge density must be correctly included in both the equation for the correlation function as well as the modified PB equation (see Eq.(5.8)). These effects could be quite important in driving up the charge compensation factor θ. Consequently, we hope to include chemi-adsorption in a modified WKB like

approximation and its interplay with correlation and image effects in future work. For divalent ions, with chemi-adsorption close to the macro-ion surface, such modified WKB like approximation, which takes account of a surface layer, might work well for DNA surface charge densities, provided that chemi-adsorption is sufficiently large.

A second missing ingredient is a full treatment of the finite size effects of the small ions. Already, we have looked at the finite size of the charge distribution of ions, which seems very important for the correlation effects. Also, we have considered a minimum closest approach for an ion. However, steric/short range potentials should be included consistently in the statistical mechanical model. In the simplest approximation, each ion may be treated as a hard sphere, but not just at the surface of the macro-ion, in the solution as well. The hard core radius of each ion in solution may be taken to be that of the ion and a tightly bound first hydration shell of water. We are currently developing techniques to account for this in the field theoretical approach. The goal being to develop a type of equation similar to that considered in [43], modified to take account of weak correlation effects. However, we want develop this from a more rigorous statistical mechanical approach, for the macro-ion-electrolyte system, than a lattice gas. This equation should include both correlation and image charge effects (through coupling to an equation describing the correlation function).

In addition, to go beyond the Hartree equations such steric effects are essential. One can show that the correction to the Hartree approximation, for point charges without steric effects, is highly divergent. This is manifestation of the Bjerrum instability towards the formation of Bjerrum pairs. Therefore, to calculate a meaningful correction, steric effects are essential; the hard core size of the ion acts as a cutoff. Indeed, there should be a very important interplay between effective size of ions and the validity of the Hartree approximation on its own. If the hard core radius of an ion is too small, then the Hartree approximation will not work and a large proportion of ions will form electrically neutral bound Bjerrum pairs. These considerations should also be important in looking a strong coupling expansion [3,10] in the presence of salt.

Of course, our description solvent may be too simple; a constant bulk dielectric. So another direction of development would be to consider modeling the solvent in a more sophisticated way. This might be achieved through two possible routes. The first is to treat the solvent explicitly as individual dipoles. It is certainly possible to include the solvent explicitly in the field theory a single fluctuating field [19]. The problem with this approach, in water (or other strong polar solvents) is that the dipoles interact strongly (highly correlated) so one would have to go very much beyond the mean field approach. Finite size steric effects of the water molecules would also need to be considered. Though, solving the simpler problem of ions in a dilute weak polar solvent may still be insightful [19]. A second approach, more phenomenological, would be to couple the counter-ion to a Landau-Ginzburg model, describing a local polarizability field [17,18]. Such a model has enjoyed some success in describing the microscopic electrostatic effects of water [17]. Whatever the approach used, this course of study is likely to be very involved, and should be left till later in the development of the theory.

9. Conclusion and Outlook.

In this work we have developed a field theoretic formalism to handle four effects that go beyond the simple PB approach. Namely, these are image charge effects of the small ions, weak correlation effects, finite ionic charge distributions and chemi-adsorption. From this field theory we have derived self-consistent (Hartree) equations; a modified PB equation and an equation for the correlation function of a fluctuating field, which describes the additional correlation effects and image charge effects. To obtain approximate solutions to these equations we have developed a WKB like approximation.

Furthermore, we have approximated the solution to such equation for a uniform distribution of fixed charges, without chemi-adsorption, using the WKB like approximation for the correlation function. We have done this for point charges and spherically symmetric charge distributions of small univalent ions. Here, we have shown that WKB like approximation works well compared to Hartree result. Also, we have seen interplay between image charge effects, correlations and finite size effects. The image charge effects have the tendency to reduce the local concentration of ions near the surface of the macro-ion, pushing ions away. Whereas, correlation effects have the opposite effect; pushing up the concentration by drawing small ions to the surface. Increasing the size of ionic charge distributions significantly diminishes both these two effects.

We find that for the distribution of ions there are two regimes depending on the surface charge density. When the surface charge is low, the local concentration of ions is dominated by image charge repulsion and so diminishes as we move close to the surface of the macro-ion. As we increase the macro-ion charge density we move into a regime where correlation effects win out over image charge effects and the local concentration of ions increases slightly more than what the PB equation predicts due to correlation effects as one moves towards the surface of the macro-ion. We also calculate the charge compensation parameter θ for an analytical expression for the effective interaction between two cylinders.

In following publications we hope to investigate chemi-adsorption and the effect of including steric interactions between ions. Also, it will be interesting to apply what is learnt to distributions of helical charge. Here, from our microscopic theory, we would want calculate the helical moments (KL parameters) presented in [1]. Finally, we will want to consider the Hartree approximation of a system of two macro-ions to examine the validity of the effective KL theory for helical molecules [1] and where appropriate modify the KL theory to take account of correlation effects and counter-ion readjustment.

Acknowledgments

D.J. lee would like to acknowledge the support of the Max-Planck Institute for the Physics of Complex Systems.

[1] A.A Kornyshev, D. J. Lee, S. Leikin, A. Wynveen, Rev. Mod. Phys. **79**, 943 (2007); and references contained therein.
[2] A. Naji, A. Arnold, C. Holm, R. R. Netz, Europhys. Lett. **67**, 130 (2004)
[3] A. Naji and R. R. Netz, Eur. Phys. J. E, **13,** 43 (2004)
[4] R. E. Goldestanian and T. B. Liverpool, Phys. Rev. E, **66** 051802 (2002)

[5] A. Naji, S. Jungblut, A. G. Moreia, R. R. Netz, Physica A, **352**, 132 (2005); and references contained therein.
[6] A. W. C. Lau, P. Pincus , D. Levine, H. A Fertig, Phys Rev. E, **63,** 051604 (2001)
[7] A. Grosberg, T. Yu, T. Nguyen, B. I. Shklovskii, Rev. Mod. Phys., **74**, 329 (2002); and references contained therein.
[8] P. Grochowski, J. Trylska, Biopolymers, **89**, 93 (2007); and references contained therein.
[9] M. Deserno, M.A. Arnold, C. Holm, **36** 249 (2003)
[10] M. Kandŭc and R. Podgornik, Eur. Phys. J. E. **23**, 265 (2007)
[11] Y. Levin, Rep prog phys, **65**, 1577 (2002); and references contained therein.
[12] A. A Kornyshev and S. Leikin, J. Chem. Phys. **107**, 3656 (1997)
[13] R. Podgornik, B. Žekš, J. Chem Soc., Faraday Trans. 2 **5,** 611 (1988)
[14] S. Marčelja and N. Radic, Chem. Phys. Lett. **42**, 129 (1976)
[15]O. V.Dolgov, D. A. Kirhnitz , E. G. Maximov, Rev. Mod. Phys. , **53**, 81 (1981)
[16] A.A Kornyshev in *The Chemical Physics of Solvation*, edited by R. R Dogonadze, E. Kalman, A. A. Kornyshev and J. Ulstrup (Elsevier, Amsterdam, 1985).
[17] A. A. Kornyshev and G. Sutmann, J. Electroanalytical Chem. **450** 143 (1998)
[18] I. G. Medvedev, Rus. J. Elctrochem., **37**, 193 (2001)
[19] A. Abrashkin, D. Andelman, H. Orland, Phys. Rev. Lett., **99,** 077801 (2007)
[20] R. Kjellander, Coll. J. **69** 20 (2007)
[21] A.A Kornyshev and S. Leikin, Phys. Rev. Lett., **82** 4138 (1999)
[22] Z. J. Lian and H. R. Ma, J. Chem. Phys. **127** 104507 (2007)
[23] A.G. Moreira, R.R. Netz, Europhys. Lett., **57** 911 (2002)
[24] E. Raspuad, I. Chperon, A. Leforestier and F. Livolant, **77**, 1547 (1999)
[25] M. T. Saminathan, A. Antony, A. Shirahata, L. H. Sigal, T. Thomas and T. J. Thomas, Biochemistry, **38** 3821 (1999)
[26] I. Rouzina, V. A. Bloomfield, J. Phys. Chem. **100,** 9977 (1996)
[27] A. A. Kornyshev, D. J. Lee, S. Leikin, A. Wynveen, S. B. Zimmerman, Phys. Rev. Lett.,**95**, 148102 (2005)
[28] J. Ruiz-Chica, M.A. Medina, F. Sánchez-Jiménez, F. J. Ramirez, Biophys. J. **80** 443 (2001).
[29] A. A. Ouameur and H. A. Tajmur-Riahi, J. Biol. Chem., **279,** 42041 (2004)
[30] C. A. Davey, T. J. Richmond, Proc. Natl. Acad. Sci. U.S.A, **99,** 11169 (2002)
[31] E. Moldrheim, B. Anderson, N. A. Froystein and E. Sletten, Inorg. Chim. Acta, **273**, 41 (1998)
[32] A. A. Kornyshev, S. Leikin, Phys. Rev. E., **62**, 2576 (2000)
[33] A. A. Kornyshev, S. Leikin, S. V. Malinin, Eur. Phys. J. E.,**7,**83 (2002)
[34] A. Wynveen, D. J. Lee, A.A. Kornyshev, Eur. Phys. J. E, **16,** 303 (2005)
[35] D. J. Lee and A. Wynveen, J .Phys. Cond. Matt., **18,** 787 (2006)
[36] A. G. Cherstvy, A. A. Kornyshev, S. Leikin, J. Phys. Chem B, **108**, 6508 (2004)
[37] D. J. Lee, A..Wynveen, A. A. Kornyshev, Phys. Rev. E., **70**, 051913 (2004)
[38] A. Wynveen, D. J. Lee, A. A. Kornyshev, S. Leikin submitted to nucl. acids reasch; work in progress.
[39] T. J. Grycuk, Phys. Chem B, **106**, 1434 (2002)
[40] D. C. Rau and V. A. Parsegian, Biophys. J. **61** 246 (1992)
[41] A. Wynveen and F. Bresme, J. Chem. Phys, **124** 104502 (2006)
[42] F. Bresme and A, Wynveen, J. Chem. Phys, **126**, 044501 (2007)
[43] I. Borukhov, D. Amdelman and H. Orland, Electrochim. Acta **46**, 221 (2000)
[44] R.R. Netz and H. Orland, Eur. Phys. J. E., **1,** 203 (2000)
[45] S. L. Carnie, G. M. Torre, *Advances in chemical physics, Vol 56*; edited by L. Prigogine, S. A. Rice (Wiley, New York, 1984).
[46] D. J. Amit, Field Theory, *the Renormalization Group, and Critical Phenomena* (world scientific, London, 1989)
[47] We will handle the case of chemi-adsorption in a later publication.
[48] This mechanism has been discussed in the case of a Wigner crystal [A. Grosberg, T. Yu, T. Nguyen, B. I. Shklovskii, Rev. Mod. Phys., **74**, 329 (2002)], and in such an extreme case may lead to over charging.
[49] Though, we should point out that these equations will have greatest application when one considers non-symmetric ions. One may also consider polar molecules.

[50] The correlation parameter appears much larger than that what it would be in [R.R. Netz and H. Orland, Eur. Phys. J. E., **11,** 301 (2003)] ($\Xi \approx 3$), due to the difference of a factor of 2π in the definition.
[51] R. J. F. Leote de Carvalho, E. Trizac, J. P. Hansen, Phys. Rev. E, **61**, 1634 (2000)

[52] In particular, the value $r_{ion} = 0.185$ was chosen due to $\sqrt{\langle r^2 \rangle_f} = 1\text{Å}$ (for $\mu = 2.2\text{Å}$), the size of a typical ion, where $\langle g(\mathbf{r}) \rangle_f = \int d^3 r f(\mathbf{r}) g(\mathbf{r})$ and $f(\mathbf{r})$ is defined through Eq. (6.7). Though, strictly, care should taken in relating r_{ion} to ion size.

[53] It is probable that such 'over-screening' phenomena could very much depend on the choice of charge distribution and may require careful investigation.
[54] For spermine and other polyamides, the physics could be quite complicated as spermine forms a flexible rod along which four unit positive charges are distributed equally. To take account of the flexibility requires more degrees of freedom to be assigned to each molecule.
[55] Though this indeed happens in DNA for strongly adsorbed ions But this later situation can probably also be considered in a binding energy (which takes account of the removal of closely bound water) at $r = a$, right at the surface of the macro-ion.